Earth and Planetary Science Letters xxx (2010) xxx–xxx

Contents lists available at ScienceDirect

Earth and Planetary Science Letters

journal homepage: www.elsevier.com/locate/epsl

Subduction controls of Hf and Nd isotopes in lavas of the Aleutian island arc

G.M. Yogodzinski [a,*], J.D. Vervoort [b], S.T. Brown [a,c], M. Gerseny [b]

[a] Department of Earth & Ocean Sciences, University of South Carolina, 701 Sumter St., EWSC617, Columbia, SC 29208, United States
[b] School of Earth & Environmental Sciences, Washington State University, P.O. Box 642812 Pullman, WA 99164-6376, United States
[c] Lawrence Berkeley National Laboratory, Center for Isotope Geochemistry, 1 Cyclotron Rd MS 70A-4418, Berkeley, CA 94720, United States

ARTICLE INFO

Article history:
Received 29 March 2010
Received in revised form 17 September 2010
Accepted 22 September 2010
Available online xxxx

Editor: R.W. Carlson

Keywords:
geochemistry
hafnium isotopes
neodymium isotopes
subduction
basalt
andesite
dacite

ABSTRACT

The Hf and Nd isotopic compositions of 71 Quaternary lavas collected from locations along the full length of the Aleutian island arc are used to constrain the sources of Aleutian magmas and to provide insight into the geochemical behavior of Nd and Hf and related elements in the Aleutian subduction–magmatic system. Isotopic compositions of Aleutian lavas fall approximately at the center of, and form a trend parallel to, the terrestrial Hf–Nd isotopic array with ε_{Hf} of +12.0 to +15.5 and ε_{Nd} of +6.5 to +10.5. Basalts, andesites, and dacites within volcanic centers or in nearby volcanoes generally all have similar isotopic compositions, indicating that there is little measurable effect of crustal or other lithospheric assimilation within the volcanic plumbing systems of Aleutian volcanoes. Hafnium isotopic compositions have a clear pattern of along-arc increase that is continuous from the eastern-most locations near Cold Bay to Piip Seamount in the western-most part of the arc. This pattern is interpreted to reflect a westward decrease in the subducted sediment component present in Aleutian lavas, reflecting progressively lower rates of subduction westward as well as decreasing availability of trench sediment. Binary bulk mixing models (sediment + peridotite) demonstrate that 1–2% of the Hf in Aleutian lavas is derived from subducted sediment, indicating that Hf is mobilized out of the subducted sediment with an efficiency that is similar to that of Sr, Pb and Nd. Low published solubility for Hf and Nd in aqueous subduction fluids lead us to conclude that these elements are mobilized out of the subducted component and transferred to the mantle wedge as bulk sediment or as a silicate melt. Neodymium isotopes also generally increase from east to west, but the pattern is absent in the eastern third of the arc, where the sediment flux is high and increases from east to west, due to the presence of abundant terrigenous sediment in the trench east of the Amlia Fracture Zone, which is being subducting beneath the arc at Seguam Island. Mixing trends between mantle wedge and sediment end members become flatter in Hf–Nd isotope space at locations further west along the arc, indicating that the sediment end member in the west has either higher Nd/Hf or is more radiogenic in Hf compared to Nd. This pattern is interpreted to reflect an increase in pelagic clay relative to the terrigenous subducted sedimentary component westward along the arc. Results of this study imply that Hf does not behave as a conservative element in the Aleutian subduction system, as has been proposed for some other arcs.

1. Introduction

The geochemistry of island arc lavas plays a key role in our understanding of the physical conditions in subduction zones and is fundamental to our perspectives on the genesis of continental lithosphere and the evolution of the crust–mantle system. A powerful approach to understanding subduction magmatism is through studies that link arc lava geochemistry to the physical and geological parameters of subduction in different tectonic settings. It is well known, for example, that the thickness of arc crust and mantle lithosphere contribute significantly to the geochemical features that distinguish island arc lavas from those in Andean-style, continental arcs (Hildreth and Moorbath, 1988; Leeman, 1983; Plank and Langmuir, 1988). Similarly, the age of the subducting oceanic lithosphere (Defant and Drummond, 1990), the nature of marine sediments on the subducting plate (Plank and Langmuir, 1993), the presence of back-arc spreading centers (McCulloch and Gamble, 1991), and proximity to subducting plate edges (Abratis and Wörner, 2001; Yogodzinski et al., 2001) or to mantle plumes (Turner and Hawkesworth, 1998; Wendt et al., 1997), all appear to play a significant role in controlling the geochemistry of arc lavas in different settings. Studies of arc volcanic rocks in these various subduction settings therefore each provide unique insights about the physical conditions and geochemical processes that are active in subduction systems and that control the genesis and transport of subduction magmas.

The Aleutian island arc is particularly well suited to this subduction-parameter approach to deciphering the genesis of arc lavas. This is true because the angle and rate of subduction both change

* Corresponding author. Tel.: +1 803 777 9524; fax: +1 803 777 4352.
E-mail addresses: gyogodzin@geol.sc.edu (G.M. Yogodzinski), vervoort@wsu.edu (J.D. Vervoort), stbrown@lbl.gov (S.T. Brown).

0012-821X/$ – see front matter © 2010 Elsevier B.V. All rights reserved.
doi:10.1016/j.epsl.2010.09.035

systematically from east-to-west along the arc (Fig. 1), whereas the thickness and composition of the arc crust and the age of the subducting oceanic lithosphere are essentially constant (Kelemen et al., 2003c). This allows us to evaluate geochemical variation in Aleutian lavas as a function of (1) the rate of lithosphere subduction and (2) the rate of marine sediment delivery to the trench and (presumably) the Aleutian subduction zone. Prior studies indicate that these parameters play a strong role in controlling the trace element, isotopic, and even the major element compositions of Aleutian lavas (Kay, 1980; Kay et al., 1978; Kelemen et al., 2003c; Monaghan et al., 1987; Morris et al., 1990).

In this paper we present new Hf and Nd isotopic ratios for lavas collected from the full length of the Aleutian island arc (Table 1, Fig. 1). The goal of the paper is to characterize the source of Aleutian lavas with respect to Hf–Nd isotopes and to better understand the behavior of Hf, Nd and related elements in subduction systems.

Our results demonstrate that there is relatively little geochemical variability with respect to Hf and Nd isotopes within most volcanic systems in the Aleutians, but that arc-wide variation is substantial, and is strongly correlated with subduction rates, which decrease westward along the arc. The spatial-geochemical patterns and mass balance calculations indicate that a measurable proportion of the source of Hf and Nd and related REE and HFSEs in Aleutian lavas lies in subducted marine sediment, and that the composition of the marine sediment component shifts from dominantly terrigenous in the eastern part of the arc to an increasing pelagic clay component in the west. Consistent with previous studies and with experimental observations indicating that high field strength and rare-earth elements (HFSE and REE) are relatively insoluble in hydrous fluids (Brenan et al., 1995, Class et al., in press), these results indicate that Hf and Nd in Aleutian lavas are mobilized out of bulk sediment (Kay, 1980; Kay et al., 1978) or in a sediment-silicate melt component (Chauvel et al., 2009, Class et al., in press, Elliott et al., 1997; Plank and Langmuir, 1993, Tollstrup and Gill, 2005). In turn, and consistent with other recent studies (Carpentier et al., 2009; Chauvel et al., 2009; Marini et al., 2005; Todd et al., 2010; Tollstrup et al., 2010), these results imply that Hf is effectively mobilized from the top of the subducting plate beneath the Aleutian arc, and that the Hf isotopic compositions of Aleutian lavas are therefore not a direct reflection of Hf compositions in sub-arc mantle wedge (i.e., Hf is not a 'conservative' element Pearce et al., 1999).

2. Sample selection and background

An important goal of this project was to produce an integrated geochemical data set on samples collected from the full length of the oceanic portion of the Alaska–Aleutian subduction system (Fig. 1). Toward this goal, we have analyzed 71 Quaternary-age lavas from 19 volcanic centers from the Cold Bay area at the western tip of the Alaska Peninsula to Piip Seamount, an active sea-floor volcano near the Komandorsky Islands in the western-most arc (Fig. 1, Table 1).

The dominant rock types among Aleutian lavas are basalt, basaltic andesite and andesite (49–62% SiO_2), which define a medium-K series (Fig. 2). Twenty samples are basaltic, with SiO_2<53%. Most of these have high Al_2O_3 (>17%) and low MgO (<6%) and Mg# (Mg/Mg + Fe<0.55), and so are relatively evolved, probably having been significantly affected by crystal fractionation. Eleven samples are considered primitive (Mg#>0.60), and a majority of these (7) are andesites or dacites from the western part of the arc. Rocks of dacitic composition (SiO_2>63%) are relatively rare in the Aleutians (Kay and Kay, 1994; Myers et al., 2002; Romick et al., 1992). Our sample set includes 7 dacites from the Islands of Four Mountains, Great Sitkin, Little Sitkin and Piip (Table 1). Most of the Quaternary lavas are from centers that lie on the volcanic front, but 9 are from Bogoslof and Amak islands, which are back-arc volcanoes in the eastern part of the study area (Kay and Kay, 1994; Marsh and Leitz,

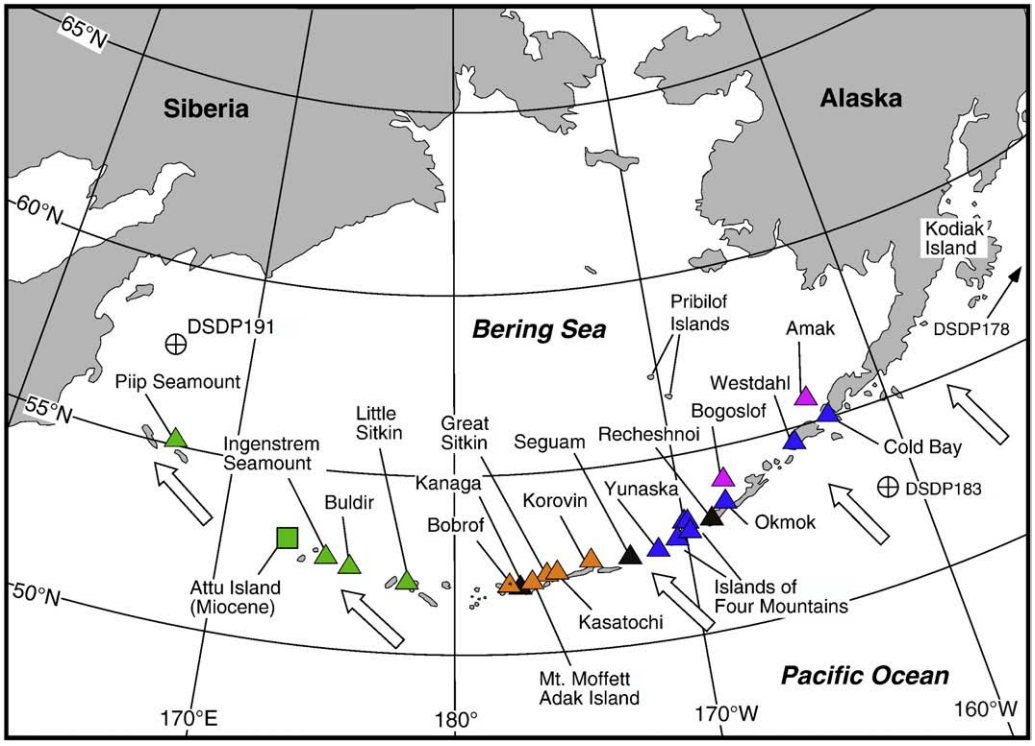

Fig. 1. Map of the Aleutian–Bering Sea region showing the names of key geographic features mentioned in the text. Colored triangles mark sample locations at Quaternary Aleutian volcanoes. The square symbol at approximately 173° E longitude marks the location Miocene-age lavas from Attu Island that are grouped with the Quaternary lavas in this paper (e.g., Figs. 2 and 3). Large arrows south of the Aleutian–Alaska arc show the approximate Pacific–North America plate convergence directions.

Please cite this article as: Yogodzinski, G.M., et al., Subduction controls of Hf and Nd isotopes in lavas of the Aleutian island arc, Earth Planet. Sci. Lett. (2010), doi:10.1016/j.epsl.2010.09.035

Table 1
Quaternary Aleutian lava compositions.

Sample ID	Volcano	Rock name	SiO_2 (wt.%)	MgO (wt.%)	K_2O (wt.%)	Mg/Mg + Fe (Mg#)[a]	$^{176}Hf/^{177}Hf$	2σ[b]	ε_{Hf}[c]	$^{143}Nd/^{144}N$	2σ[b]	ε_{Nd}	Ref.[d]
Cold Bay Area, Alaska Peninsula (162.78°N, 55.90°W)													
CB 3	Mt. Simeon	BA	56.5	4.05	1.16	0.51	0.283118	±4	11.8	0.513008	±8	7.4	1
CB 5	Mt. Simeon	A	57.9	3.19	1.08	0.46	0.283115	±5	11.7	0.513000	±10	7.2	1
CB 7	Frosty Peak	A	59.2	2.96	1.25	0.45	0.283114	±6	11.6	0.512990	±9	7.0	1
CB 12	Frosty Peak	A	57.3	3.06	1.24	0.43	0.283119	±4	11.8	0.512996	±8	7.1	1
CB 12 (rep)							0.283117	±5	11.7				
CB 44	Morzhovoi	BA	52.4	3.26	0.81	0.38	0.283138	±6	12.5	0.512977	±4	6.8	2
CB 44 (rep)							0.283140	±4	12.5	0.513005	±4	7.3	2
Amak Island — backarc (163.16°W, 55.61°N)													
AMK 1	Amak	TA	56.6	2.36	1.88	0.39	0.283120	±6	11.9	0.513013	±8	7.5	1
AMK 2	Amak	TA	56.7	2.15	1.70	0.38				0.513011	±9	7.4	1
AMK 3	Amak	BTA	56.3	3.01	1.60	0.44	0.283126	±6	12.0	0.513026	±11	7.7	1
AMK 4	Amak	TA	58.2	2.26	1.77	0.39	0.283127	±5	12.1	0.513012	±11	7.5	1
AMK 5	Amak	BA	53.5	3.78	1.54	0.44	0.283128	±5	12.1	0.513011	±8	7.4	1
AMK 7	Amak	TA	59.1	1.46	2.28	0.34	0.283125	±5	12.0	0.513006	±10	7.3	1
Unimak Island (164.69°W, 54.53°N)													
SAR 11	Westdahl	BA	52.3	4.19	0.98	0.40	0.283154	±4	13.0	0.513073	±8	8.6	
SAR 4	Westdahl	TA	62.2	1.74	1.97	0.34	0.283148	±4	12.8	0.513076	±8	8.7	
Umnak Island (168.13°W, 53.42°N)													
UM 10	Okmok	B	51.3	7.45	0.61	0.62	0.283153	±6	13.0	0.513032	±6	7.8	3
UM 4	Okmok	B	51.7	5.45	0.97	0.52	0.283149	±5	12.9	0.513054	±7	8.3	3
UM 22	Okmok	B	51.3	4.91	0.53	0.50	0.283154	±5	13.0	0.513046	±9	8.1	3
UM 5	Okmok	BA	53.6	4.46	0.77	0.42	0.283142	±4	12.6	0.513042	±9	8.0	3
UM 16	Okmok	BA	53.8	4.14	1.19	0.39	0.283151	±5	12.9	0.513061	±10	8.4	3
UM 11	Okmok	BA	52.6	4.00	1.22	0.37	0.283153	±6	13.0	0.513037	±15	7.9	3
Bogoslof Island — backarc (168.05°W, 53.92°N)													
BOG-3	Bogoslof	B	48.1	5.30	1.80	0.50	0.283124	±5	12.0	0.513040	±11	8.0	1
C1927	Bogoslof (1927)	B	48.6	4.54	1.75	0.52	0.283108	±6	11.4	0.513045	±9	8.1	3
47ABy103	Bogoslof (1796)	TA	61.0	1.10	2.90	0.35	0.283093	±9	10.9	0.512984	±9	6.9	3
Islands of Four Mountains (169.88°W, 52.95°N, average)													
FMI 7	Carlisle	A	59.4	3.58	1.09	0.50	0.283169	±5	13.6	0.513058	±9	8.3	3
FMI 8	Uliaga	A	60.3	2.35	1.78	0.42	0.283159	±5	13.2	0.513063	±7	8.4	3
FMI 8 (rep)							0.283153	±6	13.0				
FMI 5	Herbert	A	59.6	2.08	0.82	0.36	0.283128	±5	12.1	0.513003	±9	7.3	3
FMI 6	Chuginadak	R	70.1	0.94	2.69	0.29	0.283148	±5	12.8	0.513036	±9	7.9	3
Yunaska Island (170.76°W, 52.65°N)													
FMI 2	Yunaska	A	63.0	2.09	1.13	0.36	0.283141	±5	12.6	0.513023	±13	7.7	3
Atka Island (174.12°W, 52.30°N)													
KR01-37	Korovin	B	50.6	5.65	0.69	0.51	0.283172	±6	13.7	0.513010	±9	7.4	
KR01-37 (rep)							0.283169	±6	13.6				
KR01-6	Korovin	BA	53.1	5.09	1.30	0.50	0.283176	±4	13.8	0.513035		7.9	
KR02-74	Korovin	TA	59.2	3.50	2.34	0.48	0.283154	±5	13.0	0.513012	±6	7.5	
KR02-55	Korovin	BA	55.8	4.32	1.77	0.49	0.283171	±6	13.6	0.513026	±7	7.7	
KR01-20	Korovin	BA	53.5	3.93	1.12	0.42	0.283176	±5	13.8	0.513017	±8	7.5	
KR01-33	Korovin	BTA	55.8	2.78	1.71	0.39	0.283167	±14	13.5	0.513016	±7	7.5	
KR01-9	Korovin	TA	63.1	1.74	3.04	0.35	0.283166	±6	13.5	0.513025	±6	7.7	
KR01-24	Korovin	TD	64.1	1.47	3.31	0.34	0.283174	±6	13.8	0.513018	±7	7.6	
Kasatochi Island (175.23°W, 52.16°N)													
K-7	Kasatochi	B	49.1	8.77	0.76	0.64	0.283151	±6	12.9	0.513005	±8	7.3	3
K-7 (rep)							0.283153	±7	12.9				
Great Sitkin Island (176.10°W, 52.19°N)													
SIT80-5	Great Sitkin	BA	56.2	6.37	1.13	0.61	0.283197	±5	14.6	0.513056	±9	8.3	4
GS 727	Great Sitkin	B	49.7	5.60	0.82	0.52	0.283175	±5	13.8	0.513050	±9	8.2	5
GS723	Great Sitkin	A	61.2	2.62	1.41	0.42	0.283192	±9	14.4	0.513042	±9	8.0	5
GS725-B	Great Sitkin	BA	52.4	4.14	1.10	0.45	0.283187	±4	14.2	0.513051	±8	8.2	5
GS721B	Great Sitkin	A	59.9	3.25	1.31	0.43	0.283187	±5	14.2	0.513048	±8	8.2	5
SIT-RK4	Great Sitkin	TD	66.9	1.20	2.63	0.33	0.283155	±6	13.1	0.513023	±3	7.7	4
Adak Island (176.74°W, 51.94°N)													
MOF81-56A	Mt. Moffett	A	62.6	2.07	1.65	0.42	0.283167	±5	13.5	0.513026	±13	7.7	3
MOF81-54	Mt. Moffett	BA	56.5	4.23	1.65	0.52	0.283146	±4	12.8	0.513018	±8	7.6	3
MOF81-44	Mt. Moffett	A	57.4	3.58	1.57	0.48	0.283171	±5	13.6	0.513019	±10	7.6	3
MOF80-GL5	Mt. Moffett									0.513008	±8	7.4	
MOF81-38	Mt. Moffett	A	57.3	7.46	1.42	0.67	0.283149	±5	12.9				3

(continued on next page)

Please cite this article as: Yogodzinski, G.M., et al., Subduction controls of Hf and Nd isotopes in lavas of the Aleutian island arc, Earth Planet. Sci. Lett. (2010), doi:10.1016/j.epsl.2010.09.035

Table 1 (*continued*)

Sample ID	Volcano	Rock name	SiO_2 (wt.%)	MgO (wt.%)	K_2O (wt.%)	Mg/Mg + Fe (Mg#)[a]	$^{176}Hf/^{177}Hf$	2σ[b]	ε_{Hf}[c]	$^{143}Nd/^{144}N$	2σ[b]	ε_{Nd}	Ref.[d]
Adak Island (176.74°W, 51.94°N)													
MOF81-17	Mt. Moffett	BA	53.0	4.19	1.17	0.46	0.283161	±5	13.3	0.513008	±7	7.4	4
MOF81-15	Mt. Moffett	B	49.4	4.84	1.11	0.48	0.283150	±5	12.9	0.512998	±9	7.2	3
MOF81-18	Mt. Moffett						0.283149	±5	12.9	0.513010	±9	7.4	
MOF81-7	Mt. Moffett	BA	52.4	3.52	1.39	0.43	0.283139	±6	12.5	0.512992	±9	7.1	3
Bobrof Island (177.44°W, 51.91°N)													
BO9-6A	Bobrof	A	62.0	2.77	1.32	0.48	0.283172	±4	13.7	0.513043	±7	8.1	3,6
BO9-6A (rep)							0.283177	±4	13.9				
BO9-8A	Bobrof	BA	53.7	3.24	0.84	0.43	0.283182	±4	14.0	0.513047	±10	8.1	3,6
Little Sitkin Island (181.45°W, 51.94°N)													
LSIT04L21	Little Sitkin	B	51.8	4.63	0.71	0.48	0.283194	±8	14.5	0.513050	±12	8.2	
LSIT04L11	Little Sitkin	A	57.7	3.78	1.14	0.48	0.283184	±5	14.1	0.513038	±9	8.0	
LSIT04L32	Little Sitkin	A	57.6	3.77	1.10	0.48	0.283187	±6	14.2	0.513045	±10	8.1	
LSIT04L33	Little Sitkin	A	57.1	3.89	1.10	0.48	0.283189	±5	14.3	0.513052	±10	8.2	
LSIT04L3	Little Sitkin	BA	55.6	4.04	0.93	0.47	0.283186	±4	14.2	0.513057	±11	8.3	
LSIT04L3 (rep)										0.513047	±7	8.1	
LSIT04L18	Little Sitkin	A	58.5	3.59	1.30	0.46	0.283182	±5	14.1	0.513058	±10	8.3	
LSIT04L7	Little Sitkin	A	58.3	3.56	1.27	0.46	0.283190	±4	14.3	0.513066	±13	8.5	
LSIT04L39	Little Sitkin	A	60.1	3.27	1.35	0.46	0.283185	±5	14.1	0.513037	±9	7.9	
LSIT04L10	Little Sitkin	A	61.2	2.93	1.50	0.45	0.283190	±5	14.3	0.513062	±10	8.4	
LSIT04L49	Little Sitkin	D	65.1	2.14	1.62	0.46	0.283216	±10	15.2	0.513052	±11	8.2	
LSIT04L55	Little Sitkin	D	66.3	1.74	1.76	0.41	0.283191	±16	14.4	0.513054	±12	8.3	
Buldir Island (184.05°W, 52.34°N)													
BI9-6B	Buldir	BA	52.7	7.35	0.81	0.66	0.283192	±4	14.4	0.513089	±11	9.0	4
BI9-6B (rep)							0.283182	±4	14.0				4
BI9-4D	Buldir	BA	55.9	5.75	0.96	0.61	0.283173	±5	13.7	0.513059	±9	8.4	4
BI9-4D (rep)										0.513074	±13	8.7	4
BI9-6A	Buldir	A	61.5	3.72	1.50	0.58	0.283182	±4	14.0	0.513081	±11	8.8	4
Ingenstrem Depression (184.75°W, 52.5°N)													
70B29-1A	seamount	A	63.0	2.90	1.20	0.56	0.283202	±4	14.7	0.513081	±9	8.8	7, 8
Komandorsky Area (192.74°W, 55.40°N)													
V35-G5A	Piip Seamount	A	58.6	6.45	0.97	0.70	0.283211	±5	15.0	0.513153	±17	10.2	9
V35-G5A (rep)										0.513164	±22	10.4	9
V35-G4X1	Piip Seamount	A	57.4	6.50	1.09	0.69	0.283216	±7	15.2	0.513169	±4	10.5	9
V35-G1D	Piip Seamount	D	66.0	2.88	1.09	0.62	0.283197	±5	14.6	0.513150	±5	10.1	9
V35-G1A	Piip Seamount	D	63.3	3.20	1.20	0.61	0.283212	±5	15.1	0.513155	±6	10.2	9
V35-G2A	Piip Seamount	A	61.3	3.42	1.02	0.63	0.283200	±4	14.7	0.513163	±5	10.4	9
V35-G4A2	Piip Seamount	D	69.6	1.39	1.51	0.45	0.283206	±12	14.9	0.513152	±4	10.2	9

[a] Mg#s are calculated on a molar basis using total Fe.

[b] Errors on $^{176}Hf/^{177}Hf$ and $^{143}Nd/^{144}Nd$ represent within-run uncertainty calculated as 2σ, SE and expressed as variation in the 6th decimal place. Estimated uncertainty on $^{176}Hf/^{177}Hf$ and $^{143}Nd/^{144}Nd$ measurements, based on reproducibility and accuracy of known rock standards, is estimated to be better than ±0.5 ε units.

[c] ε_{Hf} and ε_{Nd} values are calculated using the chondritic values of $^{176}Hf/^{177}Hf = 0.282785$ and $^{143}Nd/^{144}Nd = 0.512630$ (Bouvier et al., 2008).

[d] Full major element compositions and other original sample information may be found in 1 — Marsh and Leitz (1979); 2 — Morris and Hart (1983); 3 — Kay and Kay (1994); 4 — Kay and Kay (1985); 5 — Neuweld (1987); 6 — Kay et al. (1982); 7 — Scholl et al., 1976; 8 — Kelemen et al. (2003a,b,c).; and 9 — Yogodzinski et al. (1994). Major element data from Yogodzinski et al. (1994) are recalculated on an anhydrous basis. Major element data for most samples with no source indicated are included in the appendix to this paper.

1979; Morris and Hart, 1983). These basalts and andesites are slightly K-rich (Fig. 2) with trachytic compositions based on their total alkali and SiO_2 contents (Table 1). Lavas included in this study are also from volcanoes that display both calc-alkaline and tholeiitic igneous series (Miyashiro, 1974). Samples from Piip ($n = 6$) and Little Sitkin ($n = 12$) define calc-alkaline trends, that clearly distinguish them from Korovin ($n = 8$), which is transitional, and from Okmok Volcano ($n = 6$), which is tholeiitic (Fig. 2 and cf., Kay et al., 1982).

Phenocrysts in Aleutian lavas are texturally and compositionally diverse and play an important role in developing models for Aleutian magma genesis (Brophy, 1987; Kay and Kay, 1985, 1994; Myers and Marsh, 1987; Yogodzinski and Kelemen, 1998). Primitive Aleutian basalts and picrites with high MgO (>8%) and Mg# (>0.70) may contain phenocrysts of olivine only (Kay et al., 1982; Nye and Reid, 1986), but such primitive lavas are relatively rare. Most Aleutian basalts contain phenocrysts of plagioclase and olivine ± clinopyroxene. In basaltic andesites, andesites, and dacites, the dominant phenocryst minerals are plagioclase, clinopyroxene, orthopyroxene and Fe–Ti oxides. Pigeonite is observed primarily in evolved lavas of tholeiitic affinity (Kay and Kay, 1985, 1994). Hornblende is relatively uncommon in Aleutian lavas, and is observed primarily in andesites and dacites from the central and western parts of the arc (e.g., at Moffett, GreatSitkin, Buldir and Piip, Kay and Kay, 1985, 1994; Yogodzinski et al., 1994). Disequilibrium phenocryst textures provide abundant evidence that Aleutian magmas are often mixed. This is particularly evident in lavas from calc-alkaline centers, where magma mixing plays a role in virtually all models for the genesis of Aleutians lavas (Brophy, 1987; Kay and Kay, 1985, 1994; Myers and Marsh, 1987; Yogodzinski and Kelemen, 1998).

We have also analyzed Miocene and Paleogene-age rocks from Attu (Yogodzinski et al., 1993), a volcanically inactive island in the western part of the arc (Fig. 1), as well as DSDP and Bering Sea area basalts from the Pribilof Islands. Published data indicate that Miocene-age Attu samples are geochemically similar to Quaternary-age lavas from the western Aleutians (e.g., Fig. 7 in Kelemen et al., 2003c). For this reason we plot them along with the Quaternary lavas throughout this paper. Geochemically MORB-like tholeiites, which appear to have

Please cite this article as: Yogodzinski, G.M., et al., Subduction controls of Hf and Nd isotopes in lavas of the Aleutian island arc, Earth Planet. Sci. Lett. (2010), doi:10.1016/j.epsl.2010.09.035

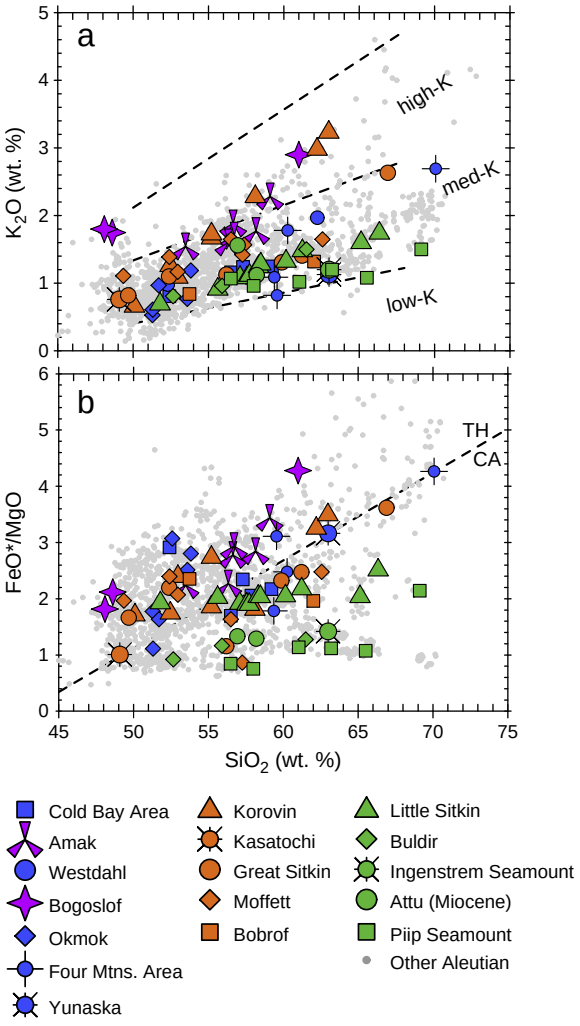

Fig. 2. Major element abundances of Aleutian lavas showing weight percent K_2O and FeO*/MgO versus SiO_2 for samples included in this study (colored symbols) compared with lava compositions compiled (in gray) by Kelemen et al. (2003c). Dashed lines separating low, medium and high-K fields in panel a are from Gill (1981). The calc-alkaline/tholeiitic discriminant line (TH/CA) in panel b is from Miyashiro (1974).

been produced by melting of Aleutian upper mantle, include the Paleogene-age basement series basalts from Attu, the DSDP 191 basalt from the western Bering Sea, and basalt sample 2316-5, which is from the Bering Sea crust in the vicinity of Piip Seamount (Fig. 1, Table 2). Paleocene–Eocene age basalts from DSDP Sites 183 and 178 have somewhat elevated abundances of K, Ba, Sr and Zr and low Yb compared to normal MORB, and their formation is interpreted to be related to nearby seamounts on the incoming Pacific Plate (Fig. 2, MacLeod and Pratt, 1973; Stewart et al., 1973). Samples STP-4, 9 and 14 (Kay et al., 1978) are late Cenozoic alkali basalts from St. Paul Island, in the Pribilof island group (Fig. 1).

The presence of radiogenic Pb and Be, and elevated Ba/La and low Ce/Pb and other geochemical tracers of subducted sediment (Kay et al., 1978; Miller et al., 1994; Monaghan et al., 1988; Morris et al., 1990), imply that Pacific Plate sediment is a potentially important source of Hf and Nd in Aleutian lavas. The nature of sediment entering the Aleutian trench can be inferred from studies of sediment cores taken at DSDP sites 183 and 178 (Kay and Kay, 1988; Plank and Langmuir, 1998; Vervoort et al., 2005). At Site 183, the bottom of the 350 m-deep core is in Eocene turbidites (100 m thick) derived from the Zodiak Fan off the coast of western North America (Creager and Scholl, 1973; Plank and Langmuir, 1998). These are overlain by ~33 m of greenish-gray clay, which in turn is overlain by ~200 m of volcanic ash-rich diatom ooze (Creager and Scholl, 1973; Plank and Langmuir, 1998). The section at DSDP Site 178 is composed of 780-meter thick sequence of turbidites and pelagic sediment. The Site 178 sediments are similar to those at Site 183, including a bottom sequence of silt-and-sand turbidites that are probably part of the Zodiak Fan (Plank and Langmuir, 1998). The middle part of this core (280–505 m) contains mud and silt with interbedded diatom-rich mud and diatom ooze. The uppermost 280 m, which consists of dark grey mud with glacial erratics, has probably been derived from glaciated drainages of southern Alaska and is interpreted to be representative of turbidites that are carried into the Aleutian arc by transport along the axis of the trench (Plank and Langmuir, 1998; Scholl et al., 1982). Kelemen et al. (2003c) showed that the flux of sediment to the Aleutian subduction system increases from east to west, based on calculations that combine the orthogonal subduction rate (Fig. 3A), sediment thickness, and rate of sediment addition to the accretionary prism. These calculations indicate that the sediment flux increases westward from 67 m^3 of sediment per meter of arc length per year (m^3/m/yr) at Cold Bay (163° W) to approximately 95 m^3/m/yr at Seguam (172.5° W) where the Amlia Fracture Zone enters the trench (Fig. 3B). This westward increase results from the westward-thickening wedge of trench sediment that is banked against the east-facing escarpment formed by the Amlia Fracture Zone on the subducting Pacific Plate near Seguam (Scholl et al., 1982; Singer et al., 1992). West of Seguam, the sediment flux decreases systematically along the arc to approximately 20 m^3/m/yr in the Komandorsky region (Fig. 3B).

3. Analytical methods

Isotopic compositions of Hf and Nd were determined on solutions purified by well-established ion chromatography techniques detailed elsewhere (Münker, et al., 2001; Patchett and Ruiz, 1987; Patchett and Tatsumoto, 1980; Vervoort and Patchett, 1996) which are only briefly reviewed here. Sample dissolution and column chemistry were performed in the radiogenic isotope clean laboratory at Washington State University. Samples were dissolved in a 10:1 concentrated HF–HNO_3 mixture in sealed bombs in Parr-type steel jackets in a 160 °C oven for 5–7 days. After the primary HF–HNO_3 dissolution, samples were treated successively with orthoboric acid and HCl to convert fluoride to chloride complexes. A 10% aliquot of each sample solution (~0.025 g) was reserved for trace element analysis. Hafnium and Nd fractions were separated from the remaining solution using an initial cation exchange column (Dowex AG50W-X12) that isolates Hf and the light and middle REEs from the bulk rock (Vervoort and Blichert-Toft, 1999). Hafnium was purified using LN-Spec resin, and Nd was purified using an in-house preparation of HDEHP-coated Teflon powder (Patchett and Ruiz, 1987; Patchett and Tatsumoto, 1980).

All samples were analyzed on a ThermoFinnigan Neptune Multiple-Collector-Inductively Coupled Mass Spectrometer (MC-ICP-MS) at Washington State University. Samples were diluted to 125 ppb (Hf) and 100 ppb (Nd), to match the concentrations at which the JMC475 Hf and La Jolla Nd standards were run. These concentrations yielded total ion currents of approximately 1.2×10^{-10} A for Hf and 5.8×10^{-11} A for Nd. Instrumental mass bias for all samples and standards was corrected with an exponential law and using $^{179}Hf/^{177}Hf = 0.7325$ and $^{146}Nd/^{144}Nd = 0.7219$. Seventy-nine analyses of the Hf standard JMC 475 and 70 analyses of La Jolla Nd throughout the course of this study yielded average values of $^{176}Hf/^{177}Hf = 0.282149 \pm 10$ (2 SD) and $^{143}Nd/^{144}Nd = 0.511834 \pm 14$ (2 SD). This compares to the accepted values of $^{176}Hf/^{177}Hf = 0.282160$ (Vervoort and Blichert-Toft, 1999) and $^{143}Nd/^{144}Nd = 0.511859$ (Lugmair and Carlson, 1978). Residual differences were corrected using the daily averages of JMC475 and La Jolla standards respectively. Isobaric interferences on Hf isotopes (^{176}Lu on ^{176}Hf; ^{176}Yb on ^{176}Hf; ^{180}W on ^{180}Hf) were monitored using ^{175}Lu, ^{173}Yb, and

Please cite this article as: Yogodzinski, G.M., et al., Subduction controls of Hf and Nd isotopes in lavas of the Aleutian island arc, Earth Planet. Sci. Lett. (2010), doi:10.1016/j.epsl.2010.09.035

Table 2
DSDP and Pribilof Island basalts and Miocene and older Aleutian lava compositions.

Sample ID	Location	Age	Rock name	SiO_2 (wt.%)	MgO (wt.%)	K_2O (wt.%)	Mg/Mg + Fe (Mg#)	$^{176}Hf/^{177}Hf$	2σ	ε_{Hf}	$^{143}Nd/^{144}Nd$	2σ	ε_{Nd}	Ref.
Miocene and Paleogene-Age Aleutian Lavas														
AT83	Attu Island, Mt Matthews Fm.	Miocene	A	56.9	4.59	1.56	0.57	0.283205	±5	14.9	0.513117	±15	9.5	4
AT8032	Attu Island, Mt Matthews Fm.	Miocene	A	58.2	4.44	1.12	0.58	0.283196	±6	14.5	0.513115	±8	9.5	4
AT73	Attu Island Basement Series	Paleogene	B	50.6	7.11	0.28	0.56	0.283218	±6	15.3	0.513198	±9	11.1	4
AT100	Attu Island Basement Series	Paleogene	B	55.6	3.94	0.03	0.38	0.283233	±6	15.8	0.513196	±19	11.0	4
AT101	Attu Island Basement Series	Paleogene	B	52.8	4.53	0.38	0.39	0.283248	±6	16.4	0.513187	±10	10.9	4
AT144	Attu Island Basement Series	Paleogene	B	51.5	4.96	0.32	0.42	0.283246	±5	16.3	0.513218	±9	11.5	4
Pribilof Islands, Bering Sea														
STP-4	St. Paul Island		B					0.283100	±4	11.1	0.513096	±11	9.1	
STP-9	St. Paul Island		B					0.283098	±5	11.1	0.513102	±11	9.2	
STP-14	St. Paul Island		B					0.283087	±5	10.7	0.513086	±8	8.9	
Bering Sea and Pacific Plate Crust														
2316-5	Komandorsky Basin	Cenozoic	B	50.1	8.33	1.27	0.64	0.283236	±6	15.9	0.513169	±4	10.5	
DSDP 178	Gulf of Alaska		B	48.1	8.40	0.39	0.54	0.283073	±4	10.2	0.513103	±17	9.2	6
DSDP 183	Aleutian Abyssal Plain	Paleogene	B	45.9	7.70	1.20	0.55	0.283018	±6	8.2	0.513017	±10	7.5	5
DSDP 191	Komandorsky Basin	Miocene	B	47.6	6.00	0.23	0.54	0.283262	±4	16.9	0.513192	±12	11.0	5

Rock name and Mg# information are the same as in Table 1. Paleogene-age DSDP and Attu samples are classified as basalts without regard to IUGS criteria based on SiO_2, K_2O and Na_2O which have been affected by low-grade metamorphism in these samples. All ages are estimates except DSDP191 which has been dated radiometrically (Kay et al., 1978; Stewart et al., 1973). Sample 2315-5 is a deeply weathered basalt of unknown age, collected from the Bering Sea basement rocks in the vicinity of Piip Volcano (see also Yogodzinski et al., 1994). Sources for major element data and other original sample information are 1 — Kay et al. (1978); 2 — Kay and Kay (1994); 3 — Yogodzinski et al. (1995); 4 — Yogodzinski et al. (1993); 5 — Stewart et al. (1973); and 6 — MacLeod and Pratt (1973). Major element data for samples with no source indicated are included in the appendix to this paper.

^{182}W and corrected (Vervoort et al., 2004) if they exceeded 10 ppm. Total procedural blanks determined during this study indicated sample:blank ratios from 2500:1 to greater than 10,000:1 and so were insignificant. Epsilon Hf and Nd values were calculated using chondritic values of $^{176}Hf/^{177}Hf = 0.282785$ and $^{143}Nd/^{144}Nd = 0.512630$ (Bouvier et al., 2008).

4. Results

The Hf and Nd isotopic compositions of Aleutian lavas fall approximately in the center of, and form a trend parallel to, the terrestrial and mantle arrays (Fig. 4) as defined by Vervoort et al. (1999). The range of values for Quaternary-age Aleutian lavas is approximately +11.6 to +15.2 epsilon Hf units (ε_{Hf}) and +6.8 to +10.5 epsilon Nd units (ε_{Nd}). Isotope ratios for Hf and Nd in Quaternary-age Aleutian lavas generally increase from east to west along the arc, but nearly all samples from the eastern locations have ε_{Hf} values that are lower by 1.0–1.5 units at similar ε_{Nd} compared to samples from the central and western locations (Fig. 4).

Plots of ε_{Hf} and ε_{Nd} in Quaternary lavas against location within the arc demonstrate that, as observed in a variety of other geochemical variables (Kelemen et al., 2003c), there is a strong dependence of Hf and Nd isotopic compositions on sample location (Fig 3). This pattern is clearest for Hf isotopes, which increase continuously from Cold Bay to Piip (Fig. 3a). Linear regression of the volcano-averaged Hf isotope compositions with longitude, and including data from Jicha et al. (2004), produces an adjusted R^2 value of 0.82 and an F-statistic of 77 (where the F-statistic is the variance explained by the regression divided by the variance that is not explained by the regression). This indicates that the patterns in Figures 3a and 5a have a low probability (F-significance $\sim 10^{-7}$) of having arisen by chance. The westward increase in center-averaged ε_{Nd} values west of Seguam, and including data compiled from the literature (Figs. 3b and 5b), is similarly significant (adjusted $R^2 = 0.94$, $F = 238$, F-significance $\sim 10^{-10}$). East of Seguam, the Nd isotopes are more variable and in general appear to decrease from east to west (Figs. 3b and 5b). Regression of the volcano-averaged Nd isotope and sample location data in this part of the arc (Cold Bay to Seguam/162° to 174° west) indicates that the westward decreasing pattern is not statistically significant ($R^2 = 0.16$, $F = 1.47$, F-significance = 0.26).

Variations of Hf and Nd isotopic compositions of Aleutian lavas with major element parameters (SiO_2, K_2O, Mg/Mg + Fe = Mg#) reveal patterns that are primarily indicative of the regional trend of westward increasing Hf and Nd isotopes along the arc (Fig. 6). For example, Hf and Nd are generally less radiogenic in the more evolved samples, which have lower Mg# (Fig. 6), but this mainly reflects the regional pattern toward higher ε_{Hf} and ε_{Nd} in western Aleutian sites (Piip, Attu and Buldir) where there is a higher proportion of high Mg# samples (Figs. 3 and 5). There is also no relationship between ε_{Hf} or ε_{Nd} and silica content (Fig. 6). These results illustrate no arc-wide relationship between Hf and Nd isotopic composition with rock type or other major element parameters (Fig. 6).

For volcanic centers where we have analyzed five or more lavas spanning a variety of rock types (Okmok, Korovin, Moffett, Little Sitkin and Piip), we observe only minor variability in Hf and Nd isotopes. At Korovin and Little Sitkin, andesites and dacites with $SiO_2 > 60\%$, have Hf and Nd isotope ratios that are similar to those of basalts and basaltic andesites with $SiO_2 < 56\%$ from those centers. At Piip, andesites and dacites which have the most radiogenic Hf and Nd in the arc, show a small decrease in ε_{Nd} with increasing SiO_2 and decreasing Mg#, but no change in ε_{Hf} (Fig. 6). In contrast, basalts and andesites at Mt. Moffett show a modest increase in ε_{Nd} and ε_{Hf} with increasing SiO_2, from 49 to 63% SiO_2 (Fig. 5). Otherwise we observe no systematic variation of Hf and Nd isotopes with whole-rock major element compositions for Quaternary lavas from individual Aleutian volcanoes.

Back-arc Aleutian lavas from Bogoslof and Amak volcanoes have, on average, somewhat less radiogenic Hf and Nd isotopes compared to nearby arc-front lavas. Three samples from Bogoslof each have significantly less radiogenic Hf but similar Nd isotope ratios compared to lavas at Okmok, which is the closest arc-front volcano (Fig. 3). One of the Bogoslof samples has the least radiogenic Hf and Nd among Aleutian lavas in our data set ($\varepsilon_{Hf} = +11.3$, $\varepsilon_{Nd} = +6.8$). Five samples from back-arc volcano Amak fall within a narrow range of compositions at approximately $\varepsilon_{Hf} = +12.4$ and $\varepsilon_{Nd} = +7.4$. These compositions are nearly indistinguishable from nearby arc-front lavas in the

Please cite this article as: Yogodzinski, G.M., et al., Subduction controls of Hf and Nd isotopes in lavas of the Aleutian island arc, Earth Planet. Sci. Lett. (2010), doi:10.1016/j.epsl.2010.09.035

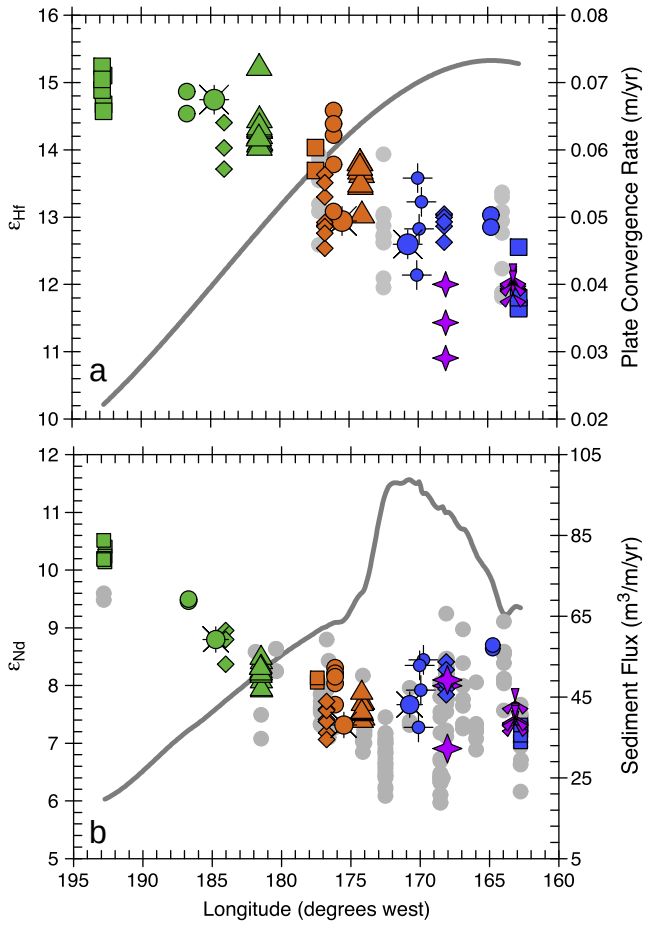

Fig. 3. Hafnium and neodymium isotopes, up-dip plate convergence, and sediment flux rates in Aleutian lava samples as a function of longitude from Cold Bay to Piip Seamount (see also Fig. 1). Colored symbols for Aleutian lavas are the same as in Fig. 2. The gray circles in panel a are Hf isotope data ($n=32$) from Jicha et al. (2004). Up-dip plate convergence rates (right scale in panel a) are from Kelemen et al. (2003c). In panel b, the gray symbols are Nd isotope data ($n=167$) compiled by Kelemen et al. (2003c) and data published more recently by Jicha et al. (2004) and Singer et al. (2007).

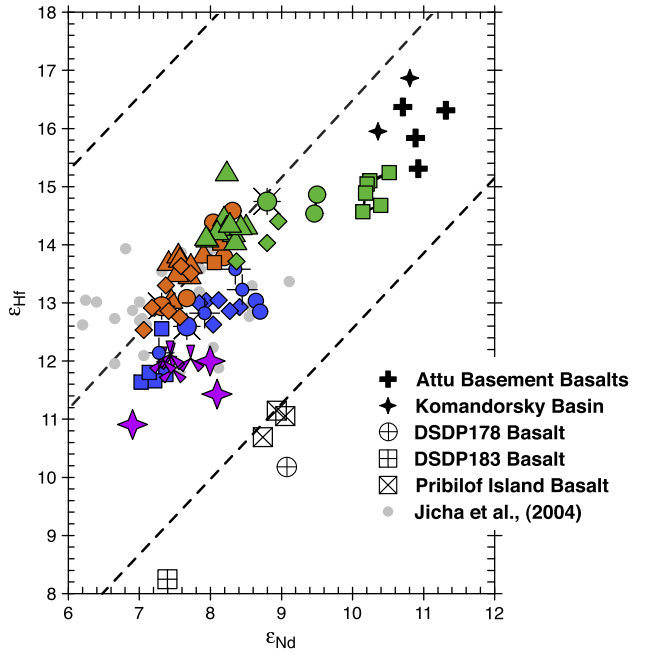

Fig. 4. Hafnium versus neodymium isotopes for Aleutian lavas and related basalts from the North Pacific and Bering Sea regions. Colored symbols are as in Figure 2. These data (except for those of Jicha et al., (2004) are from Tables 1 and 2. Diagonal dashed lines mark the Hf–Nd isotope mantle array (center line) ± 4 ε_{Hf} units (upper and lower lines) from Vervoort and Blichert-Toft (1999).

Cold Bay area (Fig. 3). Thus, there is some tendency in the back-arc data toward less radiogenic Hf compared to the arc-front (e.g., Bogoslof versus Okmok samples), but overall, the available data do not define a clear, cross-arc pattern in Hf and Nd isotopes in the eastern Aleutians, which is the only part of the arc where emergent back-arc volcanoes exist.

Basement-series tholeiitic basalts from Attu, the Komandorsky basalt collected near Piip Seamount, and the tholeiitic basalt sampled at the bottom of the DSDP drill hole 191 in the western Bering Sea (Fig. 4) have the most radiogenic Hf and Nd among samples measured (up to $+17.2$ ε_{Hf} units and $+11.5$ ε_{Nd}). These MORB-like characteristics are as expected for these samples based on their whole-rock trace element abundances and on their Pb and Sr isotope ratios (Yogodzinski et al., 1995). In contrast, alkaline-series lavas from the Pribilof Islands and from the bottoms of the DSDP drill holes on the incoming Pacific plate (holes 183 and 178) have Hf–Nd isotopic compositions that fall well off the Aleutian trend, at the bottom or below the terrestrial array between approximately $+8.2$ and $+11.0$ ε_{Hf} units, and $+7.4$ and $+9.2$ ε_{Nd} units (Fig. 4). Our calculations indicate that post-eruption growth of radiogenic Hf and Nd in Paleogene-age lavas can, at most, only account for a few tenths of an epsilon unit for Hf and Nd and therefore is not significant. The similarity of the DSDP basalt compositions to those of the Quaternary-age Pribilof basalts, suggests that both sets of lavas have sampled a north Pacific mantle source with Hf isotopic compositions that are low relative to their Nd isotopes (Fig. 4).

5. Discussion

5.1. Role of lithospheric assimilation

Limited variability in Hf and Nd isotopes within volcanic centers and between nearby centers provides a basis for concluding that, with respect to Hf and Nd, melting and assimilation of the arc crust or lithospheric mantle do not play a measurable role in the genesis of most Aleutian lavas. In general, assimilation of arc crust leading to isotopic shifts in mantle-derived melts should be most clearly expressed in evolved lavas, which have relatively high SiO_2 and low MgO and Mg# (DePaolo, 1981). Among the volcanic systems where we have isotopic data for lavas that span a substantial range of major element compositions, only those at Piip Volcano show measurable changes in Hf or Nd isotopes that are clearly correlated with SiO_2 or Mg#, and might therefore be interpreted to have been produced by assimilation of arc crust (Fig. 6c–d). The observed isotopic shift in Nd isotopes with increasing SiO_2 at Piip Volcano, however, is small (<0.6 ε_{Nd} units), and barely above the limits of analytical reproducibility. Arc wide, there is a broad pattern of relatively less radiogenic Hf and Nd with decreasing Mg# (Fig. 6b, d). This pattern, however, mostly reflects the larger proportion of high Mg# lavas from three western Aleutian locations (Attu, Buldir and Piip) which have relatively radiogenic Hf and Nd based on the regional pattern (Figs. 3 and 4).

The limited cross-arc variability is also interpreted to imply that, with respect to Hf and Nd, assimilation of crust has not had a clear influence on the geochemistry of Aleutian lavas. Specifically, back-arc lavas from Amak Volcano have Hf and Nd isotopic compositions that are nearly identical to the arc-front lavas at Cold Bay (Fig. 3). These results are consistent with published data for Pb and Sr isotopes (Morris and Hart, 1983), which indicate that there is little difference in the sources beneath the arc front and back-arc areas in this part of

Please cite this article as: Yogodzinski, G.M., et al., Subduction controls of Hf and Nd isotopes in lavas of the Aleutian island arc, Earth Planet. Sci. Lett. (2010), doi:10.1016/j.epsl.2010.09.035

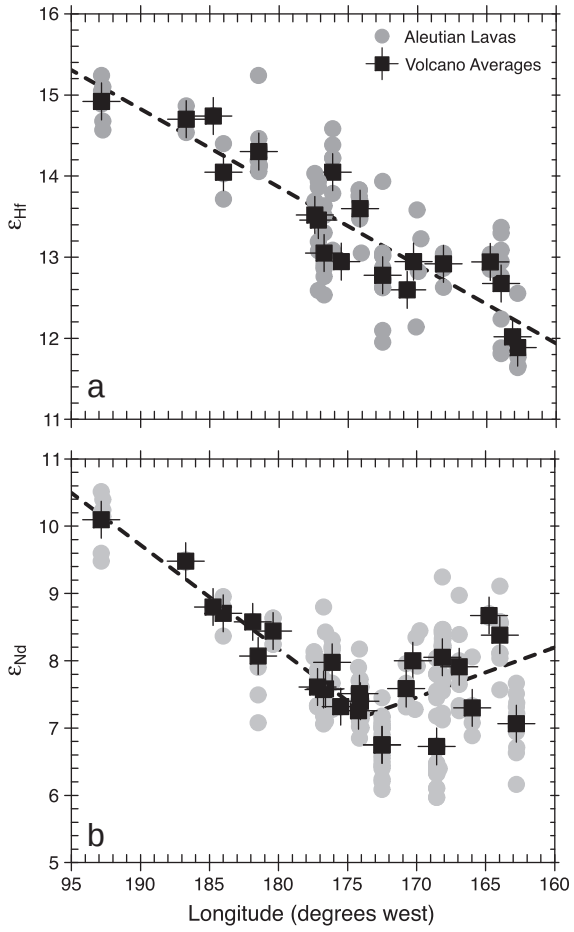

Fig. 5. Hafnium and neodymium isotopes versus Aleutian lava sample locations in degrees west longitude. Black symbols are average compositions for volcanic centers. Gray symbols are all Aleutian lavas plotted in Figure 2. Dashed lines are linear regressions through center-averaged values. In panel a the regression is through average values for the whole arc (adjusted $R^2=0.82$, $F=77$). In panel b regressions are through center-averaged values for Seguam and west (adjusted $R^2=0.94$, $F=238$) and for Seguam and east (adjusted $R^2=0.05$, $F=1.45$).

the arc. At Bogoslof we observe a small but measurable decrease in Hf and Nd isotope ratios in back-arc lavas compared to those in the arc front at Okmok (Figs. 3 and 4). This cross-arc pattern is the opposite of what we would expect if lavas from Bogoslof and Okmok were significantly affected by assimilation of arc crust. This is because Bogoslof sits primarily on oceanic crust, which should have more radiogenic Nd and Hf than the crust upon which Okmok is built, which has been thickened by at least 30–40 million years of Aleutian magmatism and accretion (Jicha et al., 2006). Published Sr isotope measurements of Bogoslof lavas (Gust and Perfit, 1987; Kay et al., 1978; von Drach et al., 1986) report relatively low values ($^{87}Sr/^{86}Sr<0.7030$) and therefore do not provide a clear basis for interpreting low ε_{Hf} values at Bogoslof (Fig. 4) to result from an unusually large component of subducted sediment in the back-arc, as has been observed at the Kasuga Seamounts compared to the arc-front volcanoes in the northern Mariana arc (Tollstrup and Gill, 2005). Melts rising below Bogoslof Volcano may have interacted with and assimilated mantle lithosphere with relatively non-radiogenic ε_{Hf}, similar in composition to the Pribilof Islands basalts (Fig. 4). Alternatively, the source of Hf in the Bogoslof lavas may lie in part in subducted seamounts with compositions similar to the DSDP 183 and 178 basalts, which have somewhat unradiogenic Hf compared to Nd and therefore lie below the mantle array (Fig. 4). This possibility is discussed further in Section 5.4.

5.2. Along-arc patterns, bulk mixing and sediment contribution estimates

The most significant geochemical patterns in our data are the along-arc changes in Hf and Nd isotopes illustrated in Figures 3 and 5. These spatial-geochemical changes are similar to those observed for other isotopic systems in the Aleutians (e.g., Fig. 7 in Kelemen et al., 2003c) and are interpreted to indicate that the main control on radiogenic isotope ratios in Aleutian lavas is the flux of marine sediment to the trench and ultimately to the melt source beneath the arc. The strong influence of subducted sediment on Aleutian lava geochemistry, and the significance of the along-arc patterns have been known for some time (Kay et al., 1978; Kelemen et al., 2003c; Monaghan et al., 1988; Morris et al., 1990; Yogodzinski et al., 1994). The importance of our results is that they include Hf isotopes for a number of samples collected in the western part of the arc (west of the Adak area), which help to clarify the westward-increasing geochemical pattern that was not clearly evident in previously available Hf isotope data (Jicha et al., 2004). This interpretation, which ties Hf in Aleutian lavas to a subducted sediment source component, implies that Hf and perhaps other HFSEs, are mobilized out of subducted sediment and incorporated into the source mixture that melted to produce the lavas. This conclusion is consistent with the limited arc-front to back-arc changes, which were noted above. These results clearly show that Hf and perhaps other HFSEs, do not exhibit conservative behavior in the Aleutian subduction zone as has been hypothesized for some other arc systems (Münker et al., 2004; Pearce et al., 1999). Combined with recent findings from other arcs, these data indicate that Hf is commonly mobilized out of the subducted sediment pile beneath a variety of island arc systems (Carpentier et al., 2009; Chauvel et al., 2009; Marini et al., 2005; Todd et al., 2010; Tollstrup and Gill, 2005; Tollstrup et al., 2010).

Mixing calculations involving mantle wedge and bulk subducted sediment end-member compositions provide additional information about the Aleutian source and processes involved in melt generation (Fig. 7). Constraints on the composition of the Aleutian mantle wedge are provided by the depleted tholeiitic basalts of the Attu basement series and by a similar basalt from DSDP 191 and sample 2316-5 from the Bering Sea crust (ε_{Hf}~16.6, ε_{Nd}~10.9, Nd/Hf~4.0, Table 2 and Yogodzinski et al., 1993). These observations of tholeiitic basalts from within and behind the arc indicate that the relative Hf and Nd abundances of typical depleted MORB mantle (Nd/Hf~3.65, Salters and Stracke, 2003; Workman and Hart, 2005) provide a good estimate for the Aleutian mantle end-member. The subducted sediment mixing end-member is provided by samples from DSDP 183 and 178 (Fig. 1), as well as other published data on Pacific marine sediment geochemistry (e.g., White et al., 1986).

Mixing our depleted Aleutian mantle with bulk sediment that has the isotopic composition and Hf and Nd abundance of the DSDP 183 weighted average and a DSDP 178 turbidite (Vervoort et al., 2005) indicates that no more than approximately 2% of the Hf and Nd in lavas from the central and eastern parts of the study area may be derived from subducted sediment (mix 1 and mix 2 in Fig. 7). This result is not significantly changed if, as has been hypothesized (Nye and Reid, 1986; Plank, 2005; Singer et al., 2007), the mantle wedge beneath the Aleutians is geochemically enriched and/or variable, resulting in a slightly higher average Nd/Hf ratio (~4.3) and higher Hf and Nd abundances, as one might expect for an enriched MORB mantle composition (~0.7 ppm Nd, ~0.16 ppm Hf). These estimates, which are based on two-component mixing (mantle + sediment) and therefore assume that there is no source for Hf and Nd in the basaltic part of the subducting oceanic crust (Class et al., in press; Elliott et al., 1997; Plank and Langmuir, 1993), are similar to prior estimates of mostly 1–4% for a bulk subducted sediment component in Aleutian lavas, based on Sr–Pb and Sr–Nd isotopes and on various trace element parameters (Kay et al., 1978; McCulloch and Perfit, 1981; Perfit and Kay, 1986; von Drach et al., 1986). These results indicate

Please cite this article as: Yogodzinski, G.M., et al., Subduction controls of Hf and Nd isotopes in lavas of the Aleutian island arc, Earth Planet. Sci. Lett. (2010), doi:10.1016/j.epsl.2010.09.035

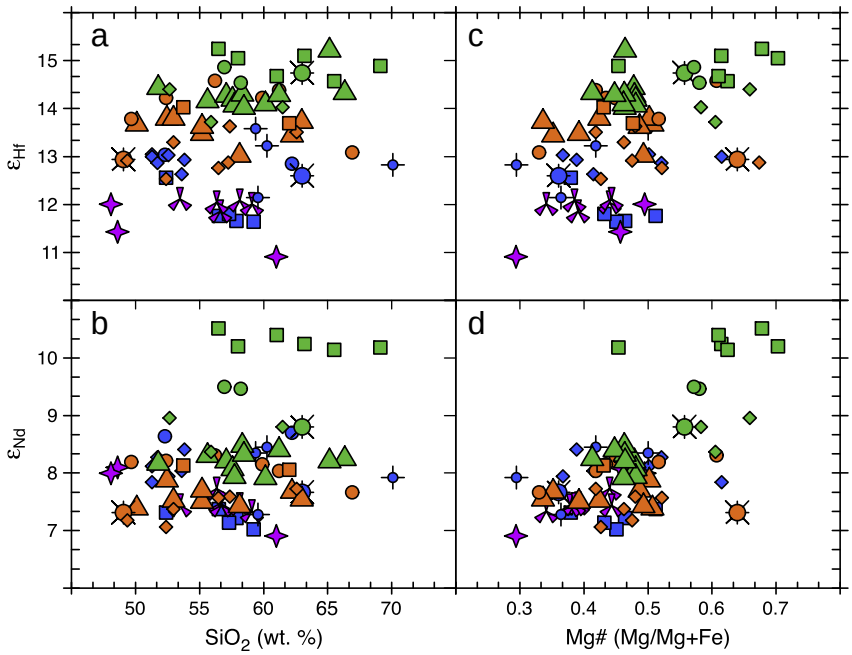

Fig. 6. Hafnium and neodymium isotopes for Aleutian lavas (Table 1) plotted against major element parameters SiO_2 (panels a–b) and Mg# (panels c–d). Calculation of Mg# is on a molar basis and includes the total whole-rock iron content. Symbols are as in Figure 2.

that Hf and Nd are mobilized out of subducted sediment with an efficiency that is broadly similar to that of Sr and Pb. This implies in turn, that the transfer of geochemical components from subducted sediment beneath arcs most likely occurs by either bulk mechanical mixing into the mantle wedge (Carpentier et al., 2009; Chauvel et al., 2009; Kay, 1980; Kay et al., 1978; Marini et al., 2005), or in the form of a silicate melt (Plank and Langmuir, 1993; Elliott et al., 1997, Class et al., in press). The possible roles of sediment melting and sediment-derived fluids versus bulk mixing are discussed further in Section 5.3.

Two-component models involving bulk-sediment that produce mixing lines that are parallel to the relatively flat trend observed in the western Aleutian lavas in Hf–Nd isotope space (Fig. 7) require a

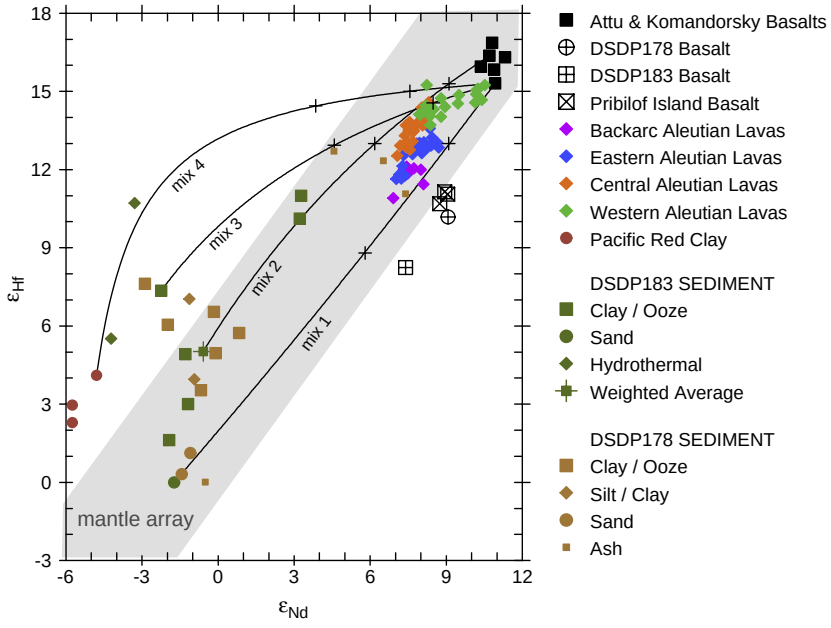

Fig. 7. Hafnium and Nd isotope compositions for Aleutian lavas compared with Pacific sediments from DSDP 183, 178 and other locations. Black lines labeled mix 1–mix 4 are binary mixing models between mantle wedge and sediment end-members. The mantle wedge end-members have Hf and Nd abundances (Hf = 0.157, Nd = 0.581) of average depleted MORB mantle from Workman and Hart (2005), which are similar to the published values for Hf and Nd in the MORB-like Attu Basement Series and Komandorsky Basin samples (Yogodzinski et al., 1993). Isotopic compositions in the mantle wedge end-members are those of AT101 (mix 1) and AT73 (mix 2–4) from Table 2. Sediment data from DSDP 183, 178 and Pacific red clay are from Vervoort et al. (2005) and White et al. (1986). The mix 1 sediment end-member has Nd = 19.4 ppm and Hf = 5.65 ppm (Nd/Hf = 3.44) is a turbidite sand from DSDP 183. The mix 2 sediment end-member is the weighted average composition for sediment in DSDP 183, (Nd = 19.07 ppm, Hf = 3.26 ppm, Nd/Hf = 5.85) from Plank and Langmuir (1998). The mix 3 sediment end-member is a clay-ooze sample from DSDP 183 with Nd = 26.4 ppm and Hf = 3.28 ppm (Nd/Hf = 8.1). The mix 4 sediment end-member is a Pacific red clay with Nd = 158 ppm and Hf = 4.40 ppm (Nd/Hf = 35.9). Crosses on the mix 1–3 lines mark the 0.5% and 2.0% sediment end-member mixtures. Crosses on the mix 4 line mark the 0.1% and 0.5% sediment end-member mixtures.

Please cite this article as: Yogodzinski, G.M., et al., Subduction controls of Hf and Nd isotopes in lavas of the Aleutian island arc, Earth Planet. Sci. Lett. (2010), doi:10.1016/j.epsl.2010.09.035

sediment end member that either lies above the mantle array (high ε_{Hf} compared to ε_{Nd}) or has somewhat elevated concentrations of Nd relative to Hf. Sediments rich in pelagic clay are present but relatively rare in both the DSDP 183 and DSDP 178 cores (Fig. 7); clay-rich pelagic sediment, however, is abundant on the Pacific plate south of the central and western Aleutians (ODP Sites 884–886, Rea et al., 1993). These sediments have not been measured for Hf–Nd isotopes, but likely have elevated Nd/Hf and relatively radiogenic Hf, perhaps approaching the compositions of the Pacific red clay analyzed by White et al. (1986) and similar pelagic sediment compositions from other western Pacific locations (Chauvel et al., 2009). A bulk mixture of Aleutian mantle with 2–3% of this type of sediment may explain the relatively flat trend of the western Aleutian lavas in Hf–Nd isotope space (mix 3 and mix 4 in Fig. 7), compared to the trend of the central and eastern Aleutian lavas (Figs. 4 and 7). Thus, Hf–Nd isotope patterns for lavas from central and eastern Aleutian Islands are consistent with a subducted sediment component that is mostly terrigenous and has a composition that lies near the center of the mantle array. Further west the subducted sediment appears to include a larger proportion of pelagic clay, which lies above the mantle array (mix 2 and 3, Fig. 7) and/or has somewhat higher Nd–Hf ratios (mix 4, Fig. 7).

This is plausible geochemically but also geologically, because an abundant source of coarse sediment is derived from southern Alaska, which is near the eastern study area, and from the Zodiac Fan, which is the large body of Paleogene-age turbidites that underlie the Aleutian Abyssal Plain in the area south of the Alaska Peninsula and eastern-most Aleutian arc (Stevenson et al., 1983). The source of the Zodiac turbidites is interpreted to be granitic and metamorphic rocks of southeastern Alaska and western British Columbia (Stewart, 1976), indicating a likely Hf–Nd isotopic composition within the terrestrial array, probably similar to Alaskan turbidites. West of 180° longitude, Aleutian trench sediments are probably less coarse and include a somewhat larger proportion of the pelagic clay component which is present on the Pacific Plate south of the central and western Aleutians (ODP Sites 884–886, Rea et al., 1993). Pelagic clays of this type generally have elevated REE abundances and Nd/Hf ratios, meaning that a small increase in the pelagic component can have a significant influence on the average subducted sediment with respect to Hf and Nd isotopes. Thus, an east-to-west change in the composition of subducted sediment, involving an increasing proportion of pelagic clay relative to terrigenous sediment, may contribute to the isotope systematics in Aleutian lavas, which show a westward flattening of data trends in Hf–Nd isotope space (Fig. 7).

5.3. Nature of the sediment component

Hydrothermal fluids might also contribute to the formation of 'flat' mixing trajectories in Hf–Nd isotope space, like those observed in our western Aleutian lavas (Fig. 7, see also Pearce et al., 1999). Experimental studies suggest, however, that the partition functions for Nd and Hf may not be sufficiently different from one another to generate elevated Nd/Hf in a slab or sediment-derived aqueous fluid (e.g., Fig. 2a in Green and Adam, 2003). Tollstrup and Gill (2005) point out that the experimental literature is actually ambiguous with respect to the relative fluid mobility of REEs and HFSEs (Ayers, 1998; Stalder et al., 1998), although more recent partitioning studies indicate that fluids at 700–800 °C and 4–6 GPa will have somewhat elevated Nd/Hf (Kessel et al., 2005).

Perhaps more important are the abundances of REEs and HFSEs in aqueous fluids equilibrated with eclogite or mantle peridotite (e.g., Fig. 12 in Grove et al., 2002) which are probably too low to have a significant impact on the Nd–Hf isotope systematics of arc lavas (Class et al., in press; Hermann et al., 2006; Tollstrup and Gill, 2005). Many cycles of fluid-fluxing could be called upon to transport Hf and Nd from the subducting plate to the mantle in quantities sufficient to impact the budgets of these elements in Aleutian lavas, but this process will also produce excessive enrichments of more fluid-soluble elements such as Ba and Pb over less soluble elements such as Th and Ce (see Fig. 12 in Kelemen et al., 2003a). In addition, recent experiments demonstrate that at 3 GPa, the water-saturated solidi for peridotite, basalt and sediment all lie between 700 and 820 °C (Hermann and Spandler, 2008; Schmidt et al., 2004; Till and Grove, 2008). These experimental results, combined with recent thermal models and related observations indicating that slab-surface temperatures beneath arcs will commonly be in this temperature range (Conder, 2005; Kelemen et al., 2003b; Plank et al., 2009; van Keken et al., in press) make it difficult to envision an intense environment of fluid-fluxing at the surface of the subducting plate in the absence of a significant melt component. Thus, it appears that aqueous fluids derived from subducted sediments may transport significant quantities of highly soluble elements, but are unlikely to transport quantities of Nd or Hf sufficient to explain Nd–Hf isotope variation in Aleutian lavas.

High Nd/Hf for the subducted sediment end-member, which is implied by the flat trajectory of the western Aleutian lava data (green symbols in Fig. 7), might also be explained by a sediment-melt component with elevated Nd/Hf. If subducted sediment is partially melted in the presence of residual zircon and/or rutile, a high ratio of Nd to Hf in the melt can be easily realized (e.g., Tollstrup and Gill, 2005). The fractionation of Nd from Hf results from the moderately strong partitioning of Zr and Hf into rutile (Foley et al., 2000) and to the high abundance of these elements in zircon. A sediment-melt component will also contain high concentrations of Nd and Hf, and so will mobilize these elements efficiently out of the surface of the subducted slab. Experimental results indicating that water-saturated melting of sediment at 3–4 GPa will commence at 700–800 °C (Hermann and Spandler, 2008; Schmidt et al., 2004), are consistent with slab-surface temperature estimates from subduction zone thermal models that invoke temperature and stress-dependent viscosities in the mantle wedge (Conder, 2005; Kelemen et al., 2003b; van Keken et al., in press). These combined experimental and modeling results indicate that melting of subducted sediment should be common in the Aleutians and in subduction zones worldwide, as predicted by various geochemical observations (Elliott et al., 1997; Plank and Langmuir, 1993) including the Hf isotope data presented here and in other recent Hf–Nd isotope studies of island arc lavas (Todd et al., 2010; Tollstrup and Gill, 2005; Tollstrup et al., 2010).

The previous discussion indicates that a sediment-melt component may be present in Aleutian lavas. Hafnium and Nd isotopes in Aleutian lavas may alternatively be explained by mixing with bulk sediment compositions, which change along the arc from dominantly terrigenous in the east to one with a stronger pelagic clay component in the west. This interpretation suggests that patterns in Hf–Nd isotope variability for island arc lavas may generally reflect not only the isotopic composition of local subducted sediment, but also the bulk Nd/Hf of that sediment. This view is consistent with data from Mariana and northern Luzon arcs in the western Pacific, where a strong pelagic clay component with high Nd/Hf is present in the subducting package, and where flat mixing trends on Hf–Nd isotope plots are common (Chauvel et al., 2009; Marini et al., 2005; Pearce et al., 1999; 2007; Todd et al., 2010; Tollstrup et al., 2010; Woodhead et al., 2001).

Sediment melting is also not necessarily consistent with the observed east-to-west changes in Hf and Nd isotopic compositions in Aleutian lavas. This is because the straight mixing lines that encompass the eastern and central Aleutian data in Figure 7 (mix 1 and 2), indicate that if the sedimentary component in the lavas was transported as a silicate melt, the melting process cannot have significantly increased Nd/Hf relative to the bulk sediment. This is also true for the mixing lines that parallel the western Aleutian data (e.g., mix 3 in Fig. 7), as long as the bulk sediment end-member in the west contains a larger pelagic clay

Please cite this article as: Yogodzinski, G.M., et al., Subduction controls of Hf and Nd isotopes in lavas of the Aleutian island arc, Earth Planet. Sci. Lett. (2010), doi:10.1016/j.epsl.2010.09.035

component than in the east. One way to reconcile the presence of a sediment-melt component with the straight mixing lines in Figure 7, and with the general success of the bulk mixing models, is to consider the possible role of residual accessory minerals such as apatite, allanite and monazite, which contain high abundances of light REEs and may therefore mitigate the effects of residual rutile and zircon which are expected to increase Nd/Hf in the sediment-melt component. This effect is well illustrated in experimentally produced hydrous melts of pelitic materials (Hermann and Rubatto, 2009) which were equilibrated with a host of accessory minerals, including zircon, apatite, monazite, allanite and phengite, but which have uniformly lower Nd/Hf (~1) than the bulk sediment from which they were melted (Nd/Hf ~4–7, Table 2 in Hermann and Rubatto, 2009).

Based on the previous discussion, it is clear that Nd and Hf isotopes and Nd/Hf ratios in Aleutian lavas may be controlled by the composition of the subducted sediment and by the presence of residual accessory minerals, including a possible role for REE-bearing phases such as allanite or monazite. It is an important point that both of these parameters (the composition of subducted sediment and the residual mineralogy) probably change from east to west along the arc, resulting from increased distances from the source of terrigenous sediment in southern Alaska, and from the changing thermal structure of the subducting plate, which is likely to be hotter to the west, due to the effects of oblique convergence and low rates of subduction.

5.4. Hf and Nd from subducted seamounts

The distinctive isotopic compositions of the DSDP 183 and 178 basalts (Fig. 4) indicate that seamount subduction may also have an effect on the Hf and Nd isotope compositions of Aleutian lavas. The most likely place for seamount subduction in the Aleutian–Alaska system is east of Cold Bay, where clusters of large seamounts in the Gulf of Alaska approach and enter the trench south and southeast of Kodiak Island (Fig. 1 in Chaytor et al., 2007). These locations are well east of our eastern-most sample locations, but local bathymetric maps also clearly show a chain of smaller seamounts southeast of Cold Bay, beginning with Derickson Seamount, which is located on the outer margin of the trench near DSDP site 183 (Fig. 1) and continuing to the SSE to other named seamounts, including Sirius, Putnam, Pritchett and Gerdes (see NOAA NOS map# 15248-14 B).

As noted previously, basalts from DSDP 183 and 178 are alkaline or transitional and as a result, appear to be related to seamounts on the incoming plate (MacLeod and Pratt, 1973; Stewart et al., 1973). These seamount-related basalts are unlikely to be broadly representative of the Pacific crust being subducted beneath the Aleutians; if subducted, however, their distinctive compositions (Fig. 4) could create a point-source geochemical component with low ε_{Hf} compared to ε_{Nd}. The distribution of seamounts on the incoming plate indicates that this geochemical component is more likely to be present in the eastern Aleutians than the west, and that it might therefore contribute to relatively straight mixing trends observed in eastern Aleutian lavas (mix 1 in Fig. 7) compared to those in the western parts of the arc (mix 2 and 3 in Fig. 7). This would be consistent with hypothesized subducted seamount contributions to the geochemistry of arc lavas in other systems for some elements. Specifically, Ishizuka et al. (in press) linked the presence of HIMU Pb in lavas of the southern Izu–Bonin arc to the involvement of Pb derived from volcaniclastic material from subducted seamounts. Their data clearly show southward trends along the arc toward elevated values of $^{206}Pb/^{204}Pb$ (>19.0), consistent with the compositions of the seamounts on the subducting plate. Incorporation of Hf and Nd from subducted seamounts would also be consistent with recent studies indicating that subducted basalt is an important source of radiogenic Hf in many arc lavas in central Mexico and the Kurile Islands (Goldstein et al., 2007; Tollstrup et al., 2007). Thus, the previously discussed non-radiogenic Hf in lavas from Bogoslof Volcano (Fig. 4) could reflect the presence of a subducted seamount component in their source. Detailed examination of Hf–Nd isotopes and HFSE and REE geochemistry along the Alaska Peninsula and in Southern Alaska, where seamount subduction is likely to be expressed, might demonstrate that lavas from these areas contain rare earth and high field strength elements not only from subducted sediment, but also from subducted basalt.

6. Conclusions

Limited variability in Hf and Nd isotope compositions in lavas from individual or nearby volcanic centers, including back-arc versus arc-front locations, indicate that with respect to these elements, assimilation of arc crust or lithosphere within the plumbing systems of Aleutian volcanoes has little or no measurable impact on the compositions of Aleutian lavas. Strong along-arc geochemical changes indicate that Hf and Nd isotopic compositions in Aleutian lavas are mainly dependent on the rates of subduction and sediment delivery to the subduction zone, and on the composition of subducted sediment, which appears to be dominantly terrigenous in the east but shifts toward a pelagic clay composition, with higher Nd/Hf, in the western part of the arc. These results are consistent with data from western Pacific arcs where a strong pelagic clay component with high Nd/Hf is present on the subducting plate, and where flat mixing trends on Hf–Nd isotope plots are common. The presence of subducted sediment-derived Hf in Aleutian lavas indicates that Hf does not behave as a conservative element in the Aleutian subduction system. The low solubility for Hf and Nd in experimentally produced aqueous fluids indicates that these elements are probably transported either in a sediment melt component or by bulk mixing of subducted sediment into the mantle wedge. Incorporation of Hf from subducted basalt into the source of Aleutian lavas is consistent with the presence of relatively non-radiogenic Hf in some samples from the eastern Aleutians, but cannot be confirmed with the present data set.

Acknowledgements

The authors thank G. Hart and C. Knaack for technical help at the ICPMS facility at Washington State University. The cooperation of SM Kay, RW Kay and BD Marsh, who provided samples for this study, is also gratefully acknowledged. Thanks also to T. Murray and others at AVO for their generous support. Helpful reviews by R. Carlson, C. Chauvel, C. Class and an anonymous reviewer greatly improved the quality of this paper. This work was supported by National Science Foundation grants EAR-0230261 to JDV and EAR-0230145 to GMY.

Appendix A. Supplementary material

Supplementary data to this article can be found online at doi:10.1016/j.epsl.2010.09.035.

References

Abratis, M., Wörner, G., 2001. Ridge collision, slab-window formation, and the flux of Pacific asthenosphere into the Caribbean realm. Geology 29, 127–130.
Ayers, J.C., 1998. Trace element modeling of aqueous fluid–peridotite interaction in the mantle wedge of subduction zones. Contrib. Mineral. 132, 390–404.
Bouvier, A., Vervoort, J.D., Patchett, P.J., 2008. The Lu–Hf and Sm–Nd isotopic composition of CHUR: constraints from unequilibrated chondrites and implications for the bulk composition of terrestrial planets. Earth. Planet. Sc. Lett. 273, 48–57.
Brenan, J.M., Shaw, H.F., Ryerson, R.J., Phinney, D.L., 1995. Mineral–aqueous fluid partitioning of trace elements at 900 °C and 2.0 GPa: constraints on trace element chemistry of mantle and deep crustal fluids. Geochim. Cosmochim 59, 3331–3350.
Brophy, J.G., 1987. The Cold Bay Volcanic center. Aleutian volcanic arc II. Implications for fractionation and mixing mechanism in calc-alkaline andesite genesis. Contrib. Mineral. 97, 378–388.
Carpentier, M., Chauvel, C., Maury, R.C., Mattielli, N., 2009. The "zircon effect" as recorded by the chemical and Hf isotopic compositins of Lesser Antilles forearc sediments. Earth. Planet. Sc. Lett. 287, 86–99.

Please cite this article as: Yogodzinski, G.M., et al., Subduction controls of Hf and Nd isotopes in lavas of the Aleutian island arc, Earth Planet. Sci. Lett. (2010), doi:10.1016/j.epsl.2010.09.035

Chauvel, C., Marini, J.C., Plank, T., Ludden, J.N., 2009. Hf–Nd input flux in the Izu–Mariana subduction zone and recycling of subducted material in the mantle. Geochem. Geophys. Geosys. 10. doi:10.1029/2008GC002101.

Chaytor, J.D., Keller, R.A., Duncan, R.A., Dziak, R.P., 2007. Seamount morphology in the Bowie and Cobb hot spot trails. Gulf Alaska. Geochem. Geophys. Geosys. 8. doi:10.1029/2007GC001712.

Class, C., Miller, D.M., et al., in press. Distinguishing melt and fluid subduction components in Umnak Volcanics, Aleutian Arc. Geochem. Geophys. Geosys. 1. doi:10.1029/1999GC000010.

Conder, J.A., 2005. A case for hot slab surface temperatures in numerical viscous flow models of subduction zones with an improved fault zone parameterization. Phys. Earth. Planet In. 149, 155–164.

Creager, J.S., Scholl, D.W., 1973. Introduction. In: Creager, J.S., Scholl, D.W. (Eds.), Initial Reports of the Deep Sea Drilling Project, Volume 19. U.S. Government Printing Office, Washington, D.C, pp. 3–16.

Defant, M.J., Drummond, M.S., 1990. Derivation of some modern arc magmas by melting of young subducted lithosphere. Nature 347, 662–665.

DePaolo, D.J., 1981. Trace element and isotopic effects of combined wallrock assimilation and fractional crystallization. Earth. Planet. Sc. Lett. 53, 189–202.

Elliott, T., Plank, T., Zindler, A., White, W., Bourdon, B., 1997. Element transport from slab to volcanic front at the Mariana arc. J. Geophys. Res. Sol. Ea. 102 14,991–915,019.

Foley, S.F., Barth, M.G., Jenner, G.A., 2000. Rutile/melt partition coefficients for trace elements and an assessment of the influence of rutile on the trace element characteristics of subduction zone magmas. Geochim. Cosmochim. 64, 933–938.

Gill, J., 1981. Orogenic Andesites and Plate Tectonics. Springer-Verlag, New York.

Goldstein, S.L., Cai, Y.M., Langmuir, C.H., LaGatta, A., Straub, S.M., Gomez-Tuena, A., Martin-Del Pozzo, A., 2007. Evidence for slab melt contributions to the Mexican Volcanic Belt and other young hot slab arcs from Lu–Hf isotopes. Eos Trans. AGU. 88(52), Fall Meet. Suppl., Abstract V41D-0800,

Green, T.H., Adam, J., 2003. Experimentally determined characteristics of aqueous fluid from partially dehydrated mafic oceanic crust at 3.0 GPa, 650–700 °C. Eur. J. Miner. 15, 815–830.

Grove, T., Parman, S.W., Bowring, S.A., Price, R., Baker, M.B., 2002. The role of an H_2O-rich fluid component in the generation of primitive basaltic andesites and andesites from the Mt. Shasta region, N California. Contrib. Miner. 142, 375–396.

Gust, D.A., Perfit, M.R., 1987. Phase relations of a high-Mg basalt from the Aleutian Island arc: implications for primary island arc basalts and high-Al basalts. Contrib. Mineral. 97, 7–18.

Hermann, J., Rubatto, D., 2009. Accessory phase control on the trace element signature of sediment melts in subduction zones. Chem. Geol. 265, 512–526.

Hermann, J., Spandler, C.J., 2008. Sediment melts at sub-arc depths: an experimental study. J. Petrol. 49, 717–740.

Hermann, J., Spandler, C., Hack, A., Korsakov, A.V., 2006. Aqueous fluids and hydrous melts in high-pressure and ultra-high pressure rocks: implications for element transfer in subduction zones. Lithos 92, 399–417.

Hildreth, W., Moorbath, S., 1988. Crustal contributions to arc magmatism in the Andes of central Chile. Contrib. Mineral. 98, 455–489.

Ishizuka, O., Taylor, R.N., Yuasa, M., Milton, J.A., Nesbitt, R.W., Uto, K., Sakamoto, I., in press. Processes controlling along-arc isotopic variation of the southern Izu-Bonin arc. Geochem. Geophys. Geosys. doi:10.1029/2006GC001475.

Jicha, B.R., B.S., S.,, Brophy, J.G., Fournelle, J.H., Johnson, C.M., Beard, B.L., Lapen, T.J., Mahlen, N.J., 2004. Variable impact of the subducted slab on Aleutian Island Arc magma sources: evidence from Sr, Nd, Pb and Hf isotopes and trace element abundances. J. Petrol. 45, 1845–1875.

Jicha, B.R., Scholl, D.W., Singer, B.S., Yogodzinski, G.M., Kay, S.M., 2006. Revised age of Aleutian Island arc formation implies high rate of magma production. Geology 34, 661–664.

Kay, R.W., 1980. Volcanic arc magma genesis: implications for element recycling in the crust–upper mantle system. J. Geol. 88, 497–522.

Kay, S.M., Kay, R.W., 1985. Aleutian tholeiitic and calc-alkaline magma series I: the mafic phenocrysts. Contrib. Mineral. 90, 276–290.

Kay, R.W., Kay, S.M., 1988. Crustal recycling and the Aleutian arc. Geochim. Cosmochim. 52, 1351–1359.

Kay, S.M., Kay, R.W., 1994. Aleutian magmas in space and time. In: Plafker, G., Berg, H.C. (Eds.), The Geology of Alaska. Geological Society of America, Boulder, pp. 687–722.

Kay, R.W., Sun, S.S., Lee-Hu, C.N., 1978. Pb and Sr isotopes in volcanic rocks from the Aleutian Islands and Pribilof Islands, Alaska. Geochim. Cosmochim. 42, 263–273.

Kay, S.M., Kay, R.W., Citron, G.P., 1982. Tectonic controls on tholeiitic and calc-alkaline magmatism in the Aleutian arc. J. Geophys. Res. Sol. Ea. 87, 4051–4072.

Kelemen, P.B., Rilling, J.L., Parmentier, E.M., Mehl, L., Hacker, B.R., 2003a. Thermal structure due to solid-state flow in the mantle wedge beneath arcs. In: Eiler, J. (Ed.), Inside the Subduction Factory, Geophysical Monograph 138. Washington D.C, American Geophysical Union, pp. 293–311.

Kelemen, P.B., Yogodzinski, G.M., Scholl, D.W., 2003b. Along-strike variation in lavas of the Aleutian Island Arc: implications for the genesis of high Mg# andesite and the continental crust. In: Eiler, J. (Ed.), Inside the Subduction Factory, Geophysical Monograph 138. Washington D.C, American Geophysical Union, pp. 223–276.

Kelemen, P.B., Hanghøj, K., Greene, A.R., 2003c. One view of the geochemistry of subduction-related magmatic arcs, with an emphasis on primitive andesite and lower crust. In: Holland, H.D., Turekian, K.K. (Eds.), Treatise on Geochemistry. Elsevier, New York, pp. 593–659.

Kessel, R., Schmidt, M.W., Ulmer, P., Pettke, T., 2005. Trace element signature of subduction-zone fluids, melts and supercritical liquids at 120–180 km depth. Nature 437, 724–727.

Leeman, W.P., 1983. The influence of crustal structure of compositions of subduction-related magmas. J. Volcanol. Geoth. Res. 13, 561–588.

Lugmair, G.W., Carlson, R.W., 1978. The Sm–Nd history of KREEP. Proceedings of the 9th Lunar Planetary Science Conference, pp. 689–704.

MacLeod, N.S., Pratt, R.M., 1973. Petrology of volcanic rocks recovered on DSDP Leg 18. In: Weser, O.E., Musich, L.F. (Eds.), Initial Reports of the Deep Sea Drilling Projects, 18. Texas A & M University, College Station, pp. 935–945.

Marini, J.C., Chauvel, C., Maury, R.C., 2005. Hf isotope compositions of northern Luzon arc lavas suggest involvement of pelagic sediments in their source. Contrib. Mineral. 149, 216–232.

Marsh, B.D., Leitz, R.E., 1979. Geology of Amak Island, Aleutian Islands. Alaska. J. Geol. 87, 715–723.

McCulloch, M.T., Gamble, J.A., 1991. Geochemical and geodynamical constraints on subduction zone magmatism. Earth. Planet. Sc. Lett. 102, 358–374.

McCulloch, M., Perfit, M.R., 1981. $^{143}Nd/^{144}Nd$, $^{87}Sr/^{86}Sr$ and trace element constraints on the petrogenesis of Aleutian island arc magmas. Earth. Planet. Sc. Lett. 56, 167–179.

Miller, D.M., Goldstein, S.L., Langmuir, C.H., 1994. Cerium/lead and lead isotope ratios in arc magmas and the enrichment of lead in the continents. Nature 368, 514–520.

Miyashiro, A., 1974. Volcanic rock series in island arcs and active continental margins. Am. J. Sci. 274, 321–355.

Monaghan, M., Measures, C., Klein, J., Middleton, R., 1987. ^{10}Be and ^{9}Be in phenocryst and groundmass separates from Aleutian-arc volcanic rocks: implications for a magmatic origin of ^{10}Be in island-arc lavas [abs.]. Trans. Am. Geophys. Union 68, 1525.

Monaghan, M.C., Klein, J., Measures, C.I., 1988. The origin of ^{10}Be in island-arc volcanic rocks. Earth. Planet. Sc. Lett. 89, 288–298.

Morris, J.D., Hart, S.R., 1983. Isotopic and incompatible trace element constraints on the genesis of island arc volcanics from Cold Bay and Amak Island, Aleutians, and implications for mantle structure. Geochim. Cosmochim. 47, 2015–2030.

Morris, J.D., Leeman, W.P., Tera, F., 1990. The subducted component in island arc lavas: constraints from Be isotopes and B–Be systematics. Nature 344, 31–35.

Münker, C., Weyer, S., Scherer, E., Mezger, K., 2001. Separation of high field strength elements (Nb, Ta, Zr, Hf) and Lu from rock samples for MC-ICPMS measurements. Geochem. Geophys. Geosyst. 2.

Münker, C., Wörner, G., Yogodzinski, G.M., Churikova, T., 2004. Behaviour of high field strength elements in subduction zones: constraints from Kamchatka–Aleutian arc lavas. Earth. Planet. Sc. Lett. 224, 275–293.

Myers, J.D., Marsh, B.D., 1987. Aleutian lead isotopic data: additional evidence for the evolution of lithospheric plumbing systems. Gechimica. Cosmochim. Acta. 51, 1833–1842.

Myers, J.D., Marsh, B.D., Frost, C.D., Linton, J.A., 2002. Petrologic constraints on the spatial distribution of crustal magma chambers, Atka Volcanic Center, central Aleutian arc. Contrib. Mineral. 143, 567–586.

Neuweld, M.A., 1987. The petrology and geochemistry of the Great Sitkin suite: Implications for the generation of calc-alkaline magmas. Cornell University Masters Thesis, Ithaca, NY, p. 174.

Nye, C.J., Reid, M.R., 1986. Geochemistry of primary and least fractionated lavas from Okmok Volcano, central Aleutians: implications for Arc magma genesis. J. Geophys. Res. Sol. Ea. 91, 10271–10287.

Patchett, P.J., Ruiz, J., 1987. Nd isotopic ages and crust formation and metamorphism in the Precambrian of eastern and southern Mexico. Contrib. Mineral. 96, 523–528.

Patchett, J.P., Tatsumoto, M., 1980. A routine high-precision method for Lu–Hf isotope geochemistry and chronology. Contrib. Mineral. 75, 263–267.

Pearce, J.A., Kempton, P.D., Nowell, G.M., Noble, S.R., 1999. Hf–Nd element and isotope perspective on the nature and provenance of mantle and subduction components in western Pacific arc-basin systems. J. Petrol. 40, 1579–1611.

Pearce, J.A., Kempton, P.D., Gill, J.B., 2007. Hf–Nd evidence for the origin and distribution of mantle domains in the SW Pacific. Earth. Planet. Sc. Lett. 260, 98–114.

Perfit, M.R., Kay, R.W., 1986. Comment on isotopic and incompatible element constraints on the genesis of island arc volcanics from Cold Bay and Amak Island, Aleutians, and implications for mantle structure. Geochim. Cosmochim. 50, 477–481.

Plank, T., 2005. Constraints from thorium/lanthanum on sediment recycling at subduction zones and the evolution of continents. J. Petrol. 46, 921–944.

Plank, T., Langmuir, C.H., 1988. An evaluation of the global variations in the major element chemistry of arc basalts. Earth. Planet. Sc. Lett. 90, 349–370.

Plank, T., Langmuir, C.H., 1993. Tracing trace elements from sediment input to volcanic output at subduction zones. Nature 362, 739–742.

Plank, T., Langmuir, C.H., 1998. The chemical composition of subducting sediment and its consequences for the crust and mantle. Chem. Geol. 145, 325–394.

Plank, T., Cooper, L.B., Manning, C.E., 2009. Emerging geothermometers for estimating slab surface temperatures. Nat. Geosci.. doi:10.1038/ngeo614

Rea, D.K., Basov, I.A., Janecek, T.R., Arnold, E., Barron, J.A., Beaufort, L., Bristow, J.F., deMenocal, P., Dubuisson, G.J., Gladenokov, A.Y., Hamilton, T., Ingram, L., Keigwin, L.D., Keller, R.A., Kotilainen, A., Krissek, L.A., McKelvey, B., Morley, J.J., Okada, M., Olafsson, G., Owen, R.M., Pak, D., Pedersen, T.F., Roberts, J.A., Rutledge, A.K., Shilov, V.V., Snoeckx, H., Stax, R., Tiedemann, R., Weeks, R., 1993. Proceedings of the Ocean Drilling Program Volume 145. Ocean Drilling Program, College Station, TX.

Romick, J.D., Kay, S.M., Kay, R.W., 1992. The influence of amphibole fractionation on the evolution of calc-alkaline andesite and dacite tephra from the central Aleutians, Alaska. Contrib. Mineral. 112, 101–118.

Salters, V.J.M., Stracke, A., 2003. Composition of the depleted mantle. Geochem. Geophys. Geosyst. 5. doi:10.1029/2003GC000597.

Schmidt, M.W., Vielzeuf, D., Auzanneau, E., 2004. Melting and dissolution of subducting crust at high pressures: the key role of white mica. Earth. Planet. Sc. Lett. 228, 65–84.

Scholl, D.W., Marlow, M.S., MacLeod, N.S., Buffington, E.C., 1976. Episodic Aleutian Ridge igneous activity: implications of Miocene and younger submarine volcanism west of Buldir Island. Geol. Soc. Am. Bull. 87, 547–554.

Please cite this article as: Yogodzinski, G.M., et al., Subduction controls of Hf and Nd isotopes in lavas of the Aleutian island arc, Earth Planet. Sci. Lett. (2010), doi:10.1016/j.epsl.2010.09.035

Scholl, D.W., Vallier, T.L., Stevenson, A.J., 1982. Deposition and deformation of Aleutian trench deposits; intersection area with Amlia Fracture Zone (173 deg. W). Mar. Geol. 48, 105–134.
Singer, B.S., Myers, J.D., Frost, C.D., 1992. Mid-Pleistocene basalts from the Seguam volcanic center, central Aleutian arc, Alaska: local lithospheric structures and source variability in the Aleutian arc. J. Geophys. Res. Sol. Ea. 97, 4579–4586.
Singer, B., Jicha, B.R., Leeman, W.P., Rogers, N.W., Thirlwall, M.F., Ryan, J., Nicolaysen, K.E., 2007. Along-strike trace element and isotopic variation in Aleutian Island arc basalt: subduction melts sediments and dehydrates serpentine. J. Geophys. Res. Sol. Ea. 112, B06206.
Stalder, R., Foley, S.F., Brey, G.P., Horn, I., 1998. Mineral–aqueous fluid partitioning of trace elements at 900–1200 °C and 3.0–5.7 GPa: new experimental data for garnet, clinopyroxene and rutile and implications for mantle metasomatism. Geochim. Cosmochim 62, 1781–1801.
Stevenson, A.J., Scholl, D.W., Vallier, T.L., 1983. Tectonic and geologic implications of the Zodiac fan, Aleutian Abyssal Plain, northeast Pacific. Geol. Soc. Am. Bull. 94, 259–273.
Stewart, R.J., 1976. Turbidites of the Aleutian abyssal plain: mineralogy, provenance, and constraints for Cenozoic motion of the Pacific plate. Geol. Soc. Am. Bull. 87, 793–808.
Stewart, R.J., Natland, J.H., Glassley, W.R., 1973. Petrology of volcanic rocks recovered on DSDP Leg 19 from the North Pacific Ocean and the Bering Sea. In: Creager, J.S., Scholl, D.W., Supko, P.R. (Eds.), Initial Reports of the Deep Sea Drilling Project, 19. U.S. Government Printing Office, Washington D.C, pp. 615–627.
Till, C.B., Grove, T.L., 2008. New observations on the melting behaviour of H_2O-saturated mantle: applications to subduction zones. Eos. Trans. AGU 89 (53) Fall Meet. Suppl., Abstract V24B-08.
Todd, E., Gill, J.B., Wysoczanski, R.J., Handler, M.R., Wright, I.C., Gamble, J.A., 2010. Sources of constructional cross-chain volcanism in the southern Havre Trough: new insights from HFSE and REE concentration and isotope systematics. Geochem. Geophys. Geosys. 11, 31.
Tollstrup, D.L., Gill, J.B., 2005. Hafnium systematics of the Mariana arc: evidence for sediment melt and residual phases. Geology 33, 737–740.
Tollstrup, D.L., Gill, J.B., Dreyer, B., 2007. High field strength and rare earth element systematics of the Kurile arc. Eos. Trans. AGU. 88 (52) Fall Meet. Suppl., Abstract V51G-08,.
Tollstrup, D., Gill, J.B., Prinkey, D., Williams, R., Tamura, Y., Ishizuka, O., 2010. Across-arc geochemical trends in the Izu–Bonin arc: contributions from the subducting slab, revisited. Geochem. Geophys. Geosys. 11, 27.
Turner, S., Hawkesworth, C., 1998. Using geochemistry to map mantle flow beneath the Lau Basin. Geology 26, 1019–1022.
van Keken, P.E., Kiefer, B., Peacock, S.M., in press. High-resolution models of subduction zones: Implications for mineral dehydration reactions and the transport of water into the deep mantle. Geochem. Geophys. Geosys. doi:10.1029/2001GC000256.
Vervoort, J.D., Blichert-Toft, J., 1999. Evolution of the depleted mantle; Hf isotope evidence from juvenile rocks through time. Geochim. Cosmochim. 63, 533–556.
Vervoort, J.D., Patchett, P.J., 1996. Behavior of hafnium and neodymium isotopes in the crust: constraints from Precambrian crustally derived granites. Geochim. Cosmochim. 60, 3717–3723.
Vervoort, J.D., Patchett, J.P., Blichert-Toft, J., Albarède, F., 1999. Relationships between Lu–Hf and Sm–Nd isotopic systems in the global sedimentary system. Earth. Planet. Sc. Lett. 168, 79–99.
Vervoort, J.D., Patchett, J.P., Söderlund, U., Baker, M., 2004. The isotopic composition Yb and the precise and accurate determination of Lu concentrations and Lu/Hf ratios by isotope dilution using MC-ICP-MS. Geochem. Geophys. Geosys. 5, Q11002. doi:10.1029/2004GC000721, A806.
Vervoort, J.D., Yu, C., Prytulak, J., Plank, T., 2005. Pb (and Hf, Nd) isotope composition of subducting marine sediments. Eos. Trans. AGU. 86, V41D–V1499D.
von Drach, V., Marsh, B.D., Wasserburg, G.J., 1986. Nd and Sr isotopes in the Aleutians: multi-component parenthood of island-arc magmas. Contrib. Mineral. 92, 13–34.
Wendt, J.I., Regelous, M., Collerson, K.D., Ewart, A., 1997. Evidence for a contribution from two mantle plumes to island-arc lavas from northern Tonga. Geology 25, 611–614.
White, W.M., Patchett, P.J., Ben Othman, D., 1986. Hf isotope ratios of marine sediments and Mn nodules: evidence for a mantle source of Hf in seawater. Earth. Planet. Sc. Lett. 79, 46–54.
Woodhead, J., Hergt, J.M., Davidson, J.P., Eggins, S.M., 2001. Hafnium isotope evidence for 'conservative' element mobility during subduction zone processes. Earth. Planet. Sc. Lett. 192, 331–346.
Workman, R.K., Hart, S.R., 2005. Major and trace element composition of the depleted MORB mantle (DMM). Earth. Planet. Sc. Lett. 231, 53–72.
Yogodzinski, G.M., Kelemen, P.B., 1998. Slab melting in the Aleutians: implications of an ion probe study of clinopyroxene in primitive adakite and basalt. Earth. Planet. Sc. Lett. 158, 53–65.
Yogodzinski, G.M., Rubenstone, J.L., Kay, S.M., Kay, R.W., 1993. Magmatic and tectonic development of the western Aleutians: an oceanic arc in a strike-slip setting. J. Geophys. Res. Sol. Ea. 98, 11807–11834.
Yogodzinski, G.M., Volynets, O.N., Koloskov, A.V., Seliverstov, N.I., Matvenkov, V.V., 1994. Magnesian andesites and the subduction component in a strongly calc-alkaline series at Piip Volcano, far western Aleutians. J. Petrol. 35, 163–204.
Yogodzinski, G.M., Kay, R.W., Volynets, O.N., Koloskov, A.V., Kay, S.M., 1995. Magnesian andesite in the western Aleutian Komandorsky region: implications for slab melting and processes in the mantle wedge. Geol. Soc. Am. Bull. 107, 505–519.
Yogodzinski, G.M., Lees, J.M., Churikova, T.G., Dorendorf, F., Wörner, G., Volynets, O.N., 2001. Geochemical evidence for the melting of subducting oceanic lithosphere at plate edges. Nature 409, 500–504.

Please cite this article as: Yogodzinski, G.M., et al., Subduction controls of Hf and Nd isotopes in lavas of the Aleutian island arc, Earth Planet. Sci. Lett. (2010), doi:10.1016/j.epsl.2010.09.035